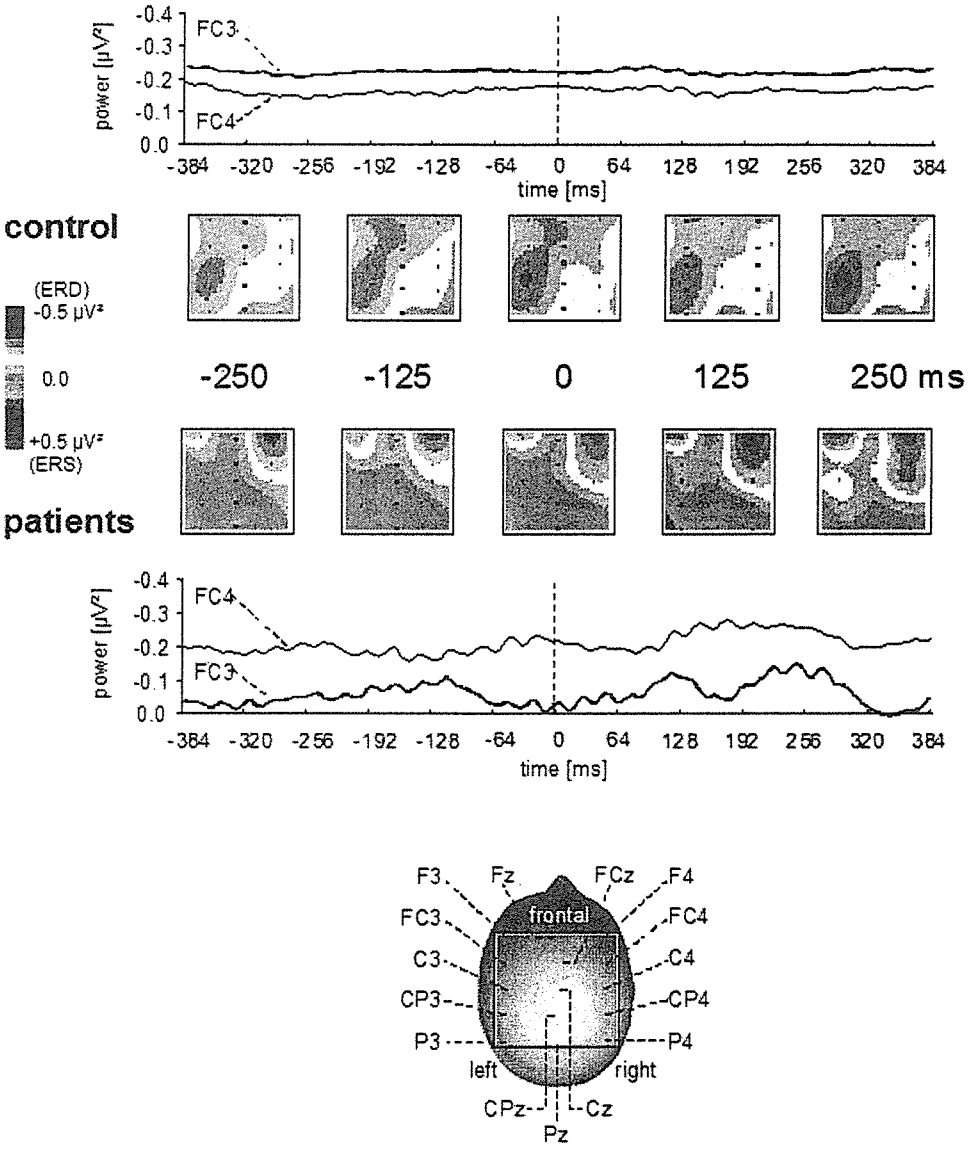

Fig. 4 Time-course analysis of spectral power in the beta band (16–20 Hz) in controls (*top row*) and stroke patients (*bottom*) (ERD). Grand average (n = 11 for each group). The curves depict the temporal evolution of ERD from 384 ms before to 384 ms after EMG onset in the central region of the lesioned (FC3) and the contralesional (FC4) central region. In normal subjects, a clear dominance of activation in the left central region (FC3 > FC4) is seen throughout the movement. In patients, the dominant activation occurs in the contralesional central region (FC4 > FC3). The topographic maps (activation coded in red) illustrate for five time points how ERD evolves in the central region (right in the map corresponds to right in the patient's brain). Note that activation of the contralesional central region in patients occurs already in the preparation phase before movement and increases slightly during movement execution. The duration of a typical EMG burst was between 200 and 350 ms. The power values on the *y*-axis are given relative to baseline (rest). Bottom = map orientation and electrode specifications.

(right). In the DAM-H, increased rCBF was found in the premotor cortex (BA 6) and medial frontal gyrus in the vicinity of the inferior frontal sulcus (BA 6). In the CON-H, increased rCBF was maximal in the PMd, (BA 6) and extended into the M1 (BA 4). Further, the right superior parietal lobule (SPL; BA 5, to a lesser extent BA 7) was more activated in patients. Finally, left cerebellar activity was higher in patients than in controls. The statistical results are given in Table 3. The topographic distribution of unequivocally enhanced activation loci in stroke patients is displayed in Fig. 6, thresholded at $Z > 3.09$. Figure 7 illustrates the details of BA 6 and BA 4 activation in the CON-H and provides an anatomical schematic on the transition between these two areas, i.e. between PMd and the corresponding parts of the M1. It is noteworthy that, the transition between these two structures varies considerably between subjects and depends on the lateral position along the central sulcus (Braak, 1979; White *et al.*, 1997; Geyer *et al.*, 2000). More medially, the M1 covers posterior aspects of the crown of the precentral gyrus, more laterally M1 tends to submerge inside the central sulcus. The co-registration plots of PET activation are given with a colour-coded scale and are thresholded at $Z > 3.09$ and

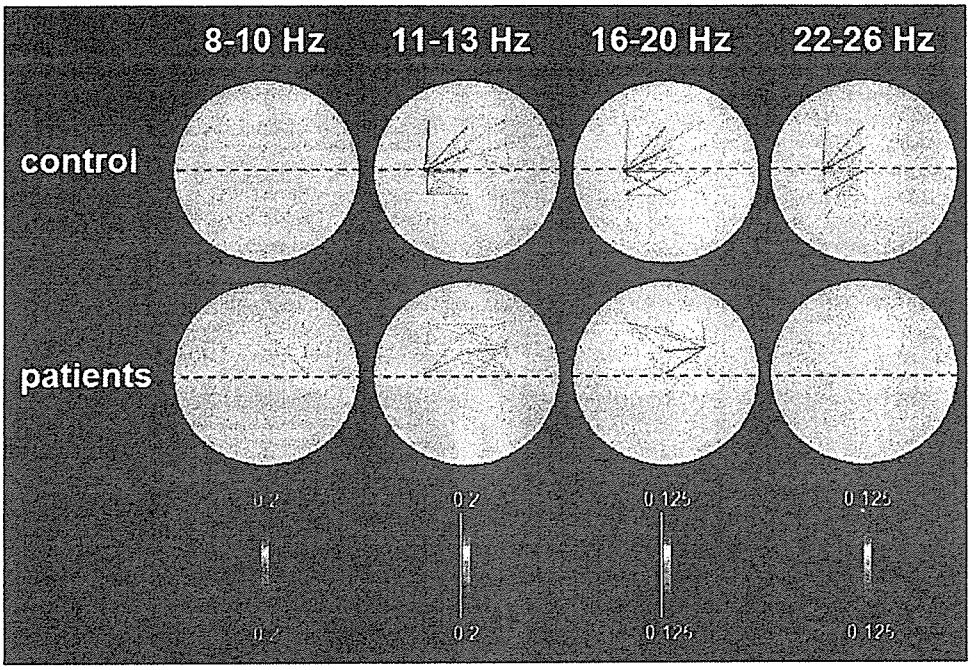

Fig. 5 Summary of functional connectivity analysis (EEG, TRCoh). Grand average (n = 11 for each group). Coherence is coded in colored links with red indicating high TRCoh increases ('enhanced synchrony') during movement. Top = in control subjects maximal functional coupling regularly occurred between the left central region and the left frontal and mesial frontocentral cortex as well as between left central and right central electrodes (11–13, 16–20, 22–26 Hz). Bottom = in patients the main difference to the normal coherence pattern was a convergence of functional links over the contralesional (right) central region. This was most prominent in the beta frequency range (16–20 Hz), indicating functional integration of the contralesional central region in the reorganized cortical network subserving motor control of the recovered hand. The dotted line indicates the anterior–posterior position of the electrodes T4, C4, Cz, C3, T3. Right-hand side of each map = right-hand side of the brain.

Table 2 Brain regions activated during right-hand movement in both patients and controls

Cerebral regions and Brodmann areas (n = 18 subjects).	Talairach-MNI coordinates (x, y, z)	t-statistic	P-value
Left central sulcus, primary motor and primary somatosensory cortex (BA 4 and BA 3)	−38, −34, 64	14.42	<0.0001
Left SMA (BA 6)	−12, 0, 66	11.39	<0.0001
Left M1 (BA 4) and left dorsal premotor cortex (BA 6)	−26, −20, 70	10.44	<0.0001
Left insula (BA 13) and basal ganglia (claustrum)	−34, −6, 8	8.25	0.001
	−32, −4, 16	7.56	0.002
Left thalamus	−12, −20, 4	7.17	0.003
	−8, −24, 10	6.56	0.010
Right anterior and posterior cerebellum	16, −56, −20	11.77	<0.0001
	40, −46, −34	7.93	<0.0001
	4, −66, −42	6.21	0.023
Left anterior and posterior cerebellum	−30, −60, −30	7.87	0.001
	−2, −72, −32	6.20	0.023
	−6, −56, −24	5.95	0.041

$Z > 2.46$. The extension of the activated area from PMd into M1 is seen at both thresholds, but more clearly in the less conservative $Z > 2.46$ map. This information has been added here because it might be important for the interpretation of diverging previous results of imaging studies with inconsistent findings regarding BA 4 (iM1) (Cramer *et al.*, 1997; Seitz *et al.*, 1998). It was noted that, the overactivation in patients inside BA 6 and BA 4 of the CON-H extended more ventrally than in the DAM-H. Also, the y- and z-coordinates of these maxima suggest that the main increase of rCBF in patients covered portions of the precentral gyrus medially adjacent to the hand knob rather than the hand knob itself.

Motor thresholds and cortical maps (TMS)

MT for the M1 of the DAM-H was significantly increased compared with the M1 of the CON-H (67.3 ± 16.8% left

Table 3 Brain regions showing significantly higher activation during right-hand movement in patients compared with control subjects

Cerebral regions and Brodmann areas	Talairach-MNI coordinates (*x*, *y*, *z*)	*t*-Statistic	*P*-value
Left premotor cortex (BA 6)	−16, −16, 76	5.16	<0.0001
Medial frontal gyrus (BA 6)	−26, 8, 30	5.03	<0.0001
Right premotor cortex (BA 6), posteriorly extending into M1 (BA 4)	14, −14, 74	4.57	<0.0001
Right SPL (precuneus, BA 5 and BA 7)	2, −40, 68	4.64	<0.0001
Left anterior cerebellum	−10, −66, −28	3.89	0.001

x, *y*, *z*-Talairach coordinates of voxels with maximal difference. *P*-value uncorrected for multiple comparisons.

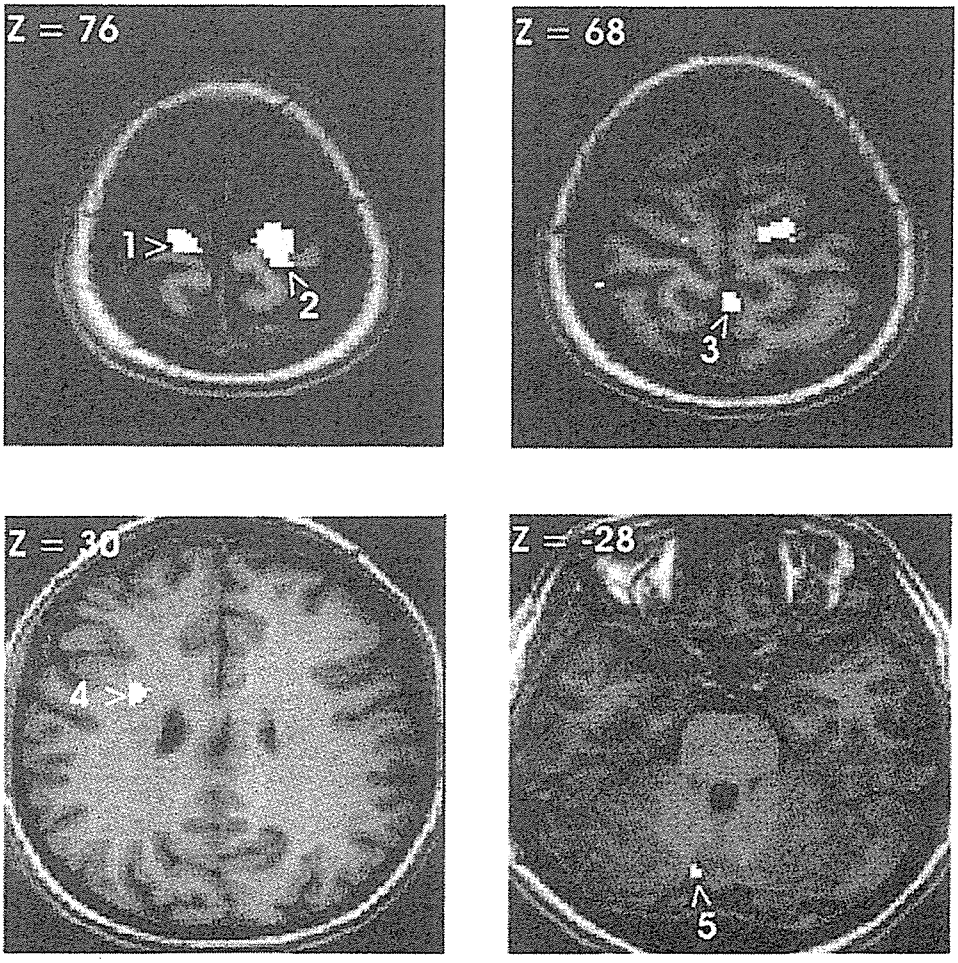

Fig. 6 Illustration of $H_2{}^{15}O$-PET results. Illustrated are the regions in which patients showed signficantly greater rCBF during right (recovered) hand movement than controls (n = 9 for each group). The regions were premotor cortex (no. 1) and medial frontal gyrus (BA 6) (#4) of the stroke hemisphere (left), premotor and M1 (no. 2) (BA 6 and BA 4) of the CON-H, SPL (no. 3) (BA 7, also BA 5) of the CON-H and left cerebellum (no. 5). z-Coordinates are given at the top left of each overlay. Images thresholded at $Z > 3.09$. Note that the location of maximum no. 4 is relatively deep, most likely at the bottom of the inferior frontal sulcus. The apparent location in the white matter in this figure is likely to be due to overlaying the group difference data on a standard anatomical brain.

versus 56.6 ± 9.4% right, Wilcoxon matched pairs test, $P < 0.05$). The results are illustrated in Fig. 8.

The *x*/*y* coordinates of the COG in the DAM-H were −5.1 ± 0.6/0.8 ± 1.3 cm, the corresponding values for the CON-H (right) were 4.8 ± 1.2/0.4 ± 1.7 cm (Wilcoxon matched pairs test, n.s.). This suggests that for MEPs elicited from the DAM-H, there was no relevant change in cortical topography of the M1 hand representation compared with the CON-H.

The NAP at the >25% level was 7.8 ± 6.7 for the DAM-H, and 7.8 ± 5.7 for the CON-H (Wilcoxon matched pairs test, n.s.). At the >50% level, the corresponding values were 4.8 ± 4.4 positions for the DAM-H, and 3.7 ± 1.8 positions for the CON-H. Although, with the strict criterion (>50%

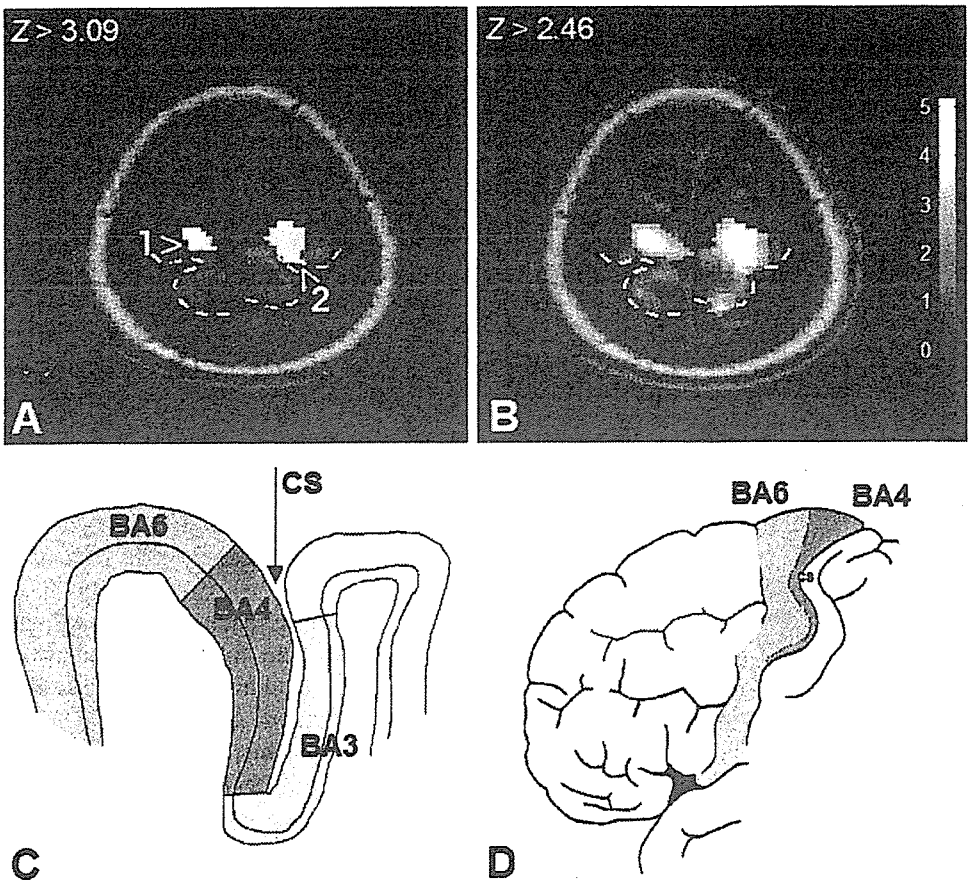

Fig. 7 Detailed illustration of enhanced rCBF during right (recovered) hand movements in stroke patients (n = 9) compared with age-matched controls (n = 9) in the contralesional central region. (**A**) image thresholded at $Z > 3.09$ (as in Fig. 6), (**B**) same image thresholded at $Z > 2.46$. Z-score colour scale is given on the right. The central sulcus is marked with a dashed white line. Note that independent of the threshold used, BA 6 activation extends into BA 4 of the CON-H. (**C**) schematic of the transition between BA 4 and BA 6. As a rule, this transition is close to the posterior limit of the precentral gyrus but varies according to the lateral position along the central sulcus (CS). This latter aspect is depicted in (**D**). The vicinity of BA 6 and BA 4 as well as the variability of the transition between the two of them might contribute to some of the inconsistencies regarding presence or absence of contralesional BA 4 activation in previous studies.

amplitude) the map size therefore tended to be slightly larger in the DAM-H, this did not reach significance because of inter-subject variability (Wilcoxon matched pairs test, P = 0.12, n.s.). In summary, there was no relevant increase or decrease of the cortical representation of hand muscles in the M1 of the DAM-H.

Most importantly, in no instance were we able to elicit MEPs in the recovered (right) hand by stimulating iM1 (at rest and with pre-contraction of the right-hand muscles).

Discussion

This study combines clinical, structural, metabolic and electrophysiological measures in a group of stroke patients with very similar subcortical lesions, clinical outcome and handedness. All patients were tested in the chronic phase after stroke, had small lesions of the posterior limb of the left internal capsule and had recovered well enough so that they could use the formerly paralysed hand for daily life activities. During all functional imaging procedures involving voluntary movement of the recovered hand, EMG was monitored bilaterally to control for mirror movements or covert involuntary co-contractions of the healthy hand. In our opinion, this is an important prerequisite for any attempt to interpret enhanced activation in the CON-H as a surrogate marker of plastic reorganization.

Although some of the data are corroborative, this study fulfils two requirements, (i) it combines a comprehensive spectrum of imaging and electrophysiological techniques in the same patients and (ii) it includes only patients with focal lesions of the posterior limb of the internal capsule in the left (dominant) hemisphere. Thereby, the present results gain additional validity as to the conclusions drawn with respect to pattern and potential functional implications of reorganization in subcortical capsular stroke.

Localization of ischaemic lesions

In all patients, the ischaemic lesion affected the posterior limb of the left internal capsule. As documented in Table 1, all but

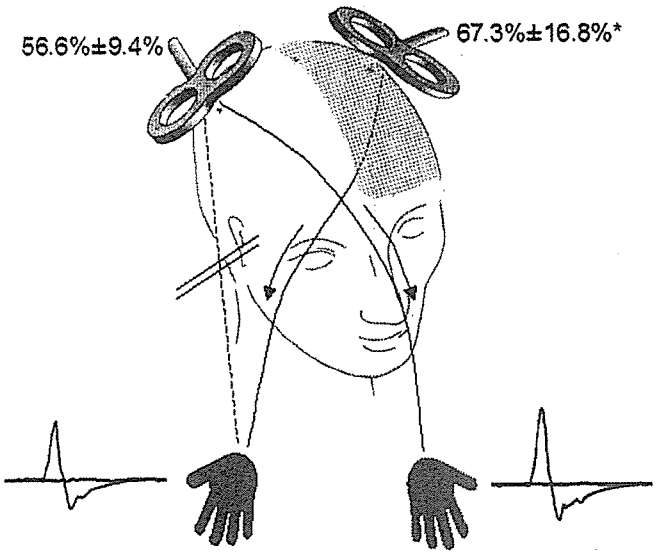

Fig. 8 Illustration of TMS data in the patient group. The stroke hemisphere is marked in yellow. The only significant difference between hand motor representations in the DAM-H and CON-H was a significantly increased MT in the affected side (*$P < 0.05$). Of note, no ipsilateral ('uncrossed') responses could be elicited in any of the patients (dashed line). Bottom right and left, two examples of MEPs.

one patient had minor additional T_1 and/or T_2 signal abnormalities which probably represented clinically inapparent ischaemic lesions in this population. These occurred mostly in the globus pallidus ($n = 7$) white matter ($n = 7$), or putamen ($n = 6$) of the left (stroke) hemisphere. None of our patients had any cortical or infra-tentorial lesions, and none had experienced previous clinical strokes or transient neurological symptoms.

Activation patterns in the CON-H (intact)

One of the major objectives of this study was to evaluate the role of the iM1, in reorganization after stroke. In our experiments, evidence for involvement of iM1 came from EEG spectral power analysis showing that the right central region was more active in patients than in controls. This result was most pronounced in the beta frequency range which is particularly sensitive to variation of motor parameters (rather than somatosensory) (Andres *et al.*, 1999; Mima *et al.*, 2001*a*; Chen *et al.*, 2003). Moreover, the time course of spectral power evolution verified that activation of the contralesional central region was present during movement preparation as well as execution. This precludes the possibility that the contralesional activation seen here was caused by altered feedback processing or reflex-like activation of the contralesional motor system by the movement as proposed previously (Verleger *et al.*, 2003). As the topographical resolution of a 28-channel surface EEG is only in the centimeter range, $H_2{}^{15}O$-PET data were obtained for assessment of metabolic changes. In line with the EEG results in the high alpha and beta bands (11–13, 16–20, 22–26 Hz), rCBF was enhanced in the frontocentral region of the CON-H. Specifically, contralesional BA 6 and BA 4 showed enhanced PET activation. In addition, the SPL including BA 5 and BA 7 exhibited higher rCBF values in patients than in the control group. This confirms that BA 4 (iM1) is reorganized during recovery from capsular stroke and is generally in line with the PET data of Nelles *et al.* (1999) and an fMRI study by Fujii and Nakada (2003). As in the EEG results which showed a more anterior distribution of the activation maxima in the CON-H than in the DAM-H, the increased rCBF in patients had its maximum in the PMd (BA 6) and extended into BA 4, as well as ventrally. As mentioned above (results section), one reason for inconsistencies regarding BA 4 activation in capsular stroke patients across multiple studies could be a different interpretation of active voxels in the vicinity of the posterior aspect of the precentral gyrus. According to several anatomical studies, M1 reaches the surface in more medial parts of the central sulcus, but submerges laterally (Braak, 1979; White *et al.*, 1997; Geyer *et al.*, 2000). In our data, the enhanced activation in this area was at the medial end of the presumed hand and arm representation in the precentral gyrus and thus certainly covered BA 4 in addition to BA 6. The greater rCBF values in the left cerebellum in our patients are in agreement with recent data of Johansen-Berg *et al.* (2002*a*), who have demonstrated with fMRI that improvements in hand function after stroke correlated with increases in activity in superior posterior regions of the cerebellar hemispheres. Thus, it appears that the CON-H and its crossed cerebellar connections can be reorganized and upregulated as a unit after capsular stroke.

The contralesional SPL also showed increased movement-related rCBF in stroke patients. This area of interest appears to be involved in the implementation of complex sensorimotor tasks, e.g. the selection of movement based on the integration of visual and somatosensory information (Tanaka *et al.*, 1996; Wexler *et al.*, 1997; Caminiti *et al.*, 1998; Catalan *et al.*, 1998). From our results, it is tempting to speculate that the SPL serves as a multimodal integration area monitoring and controlling activation of additional resources after brain lesions.

Activation patterns in the lesioned (stroke) hemisphere

Inside the DAM-H, increased (PET) activation was present in the premotor cortex (BA 6). Most previous studies have found activation in BA 6 of the DAM-H, but to varying degrees. In subcortical stroke, enhanced bilateral BA 6 activation was observed by Weiller *et al.* (1992) (10 patients) and by Calautti *et al.* (2001) (5 patients). In patients with a mixture of cortical and subcortical lesions, both bilateral (6 and 7 patients, respectively) (Chollet *et al.*, 1991; Seitz *et al.*, 1998) and only ipsilesional (8 patients) (Pariente *et al.*, 2001) overactivation of the premotor cortex was reported. In some studies, premotor activation in the DAM-H was absent (10 patients) (Cramer *et al.*, 1997) or only present in 1out of 8 patients (Weiller *et al.*, 1993). The reason for these inconsistencies remains unclear. It needs to be noted,

that also in our patients the rCBF changes in the DAM-H were less consistent with the electrophysiological data than in the CON-H. EEG showed a global reduction of activity in the central region of the stroke hemisphere. Similarly, TMS proved higher MTs in the DAM-H, confirming the observations of other authors (Thompson *et al.*, 1995; Werhahn *et al.*, 2003). As the results of PET, EEG and TMS in the CON-H were very consistent, it is unlikely that the discrepancies in the DAM-H can be attributed to the different control groups or technical issues. The increase of rCBF in patients in the DAM-H (BA 6) did not extend ventrally like in the CON-H. This difference between hemispheres might contribute to the relative shift of EEG activation patterns from DAM-H to CON-H, but it cannot explain the absolute reduction of EEG activity in the central region of the stroke hemisphere. One possibility is that PET, EEG and TMS represent activity or excitability in different, although most likely overlapping, subsets of neurons. Another explanation is that vascular autoregulation and neurovascular coupling in the DAM-H are altered after ischaemic stroke (Sette *et al.*, 1989; Dettmers *et al.*, 1993; Pineiro *et al.*, 2002).

Cortico–cortical connectivity

Inter-regional cortico–cortical connectivity was assessed by coherence analysis of the EEG data. There was a clear shift of connectivity towards the CON-H. While 29% of the 10% highest coherence links (beta frequency range, 16–20 Hz) were centered on the left hemisphere in healthy subjects, only 18% were centered over this hemisphere in stroke patients. Instead, 70% of the top 10% coherence links in patients converged over the CON-H. This strongly suggests that the CON-H is functionally integrated in the reorganized cortical network subserving right (recovered) hand movements after stroke.

The anatomical substrate of this shift could be the corpus callosum. The iM1 is connected with its homologue via transcallosal fibers (Gould *et al.*, 1986; Rouiller *et al.*, 1994), as is the premotor cortex, and there are numerous somatotopic connections between M1 and BA 6 (Wise, 1985; Wise *et al.*, 1997). Therefore, mere shifts in synaptic weights according to Hebbian rules (Hebb, 1949; Wang *et al.*, 1995) would be sufficient to account for the observed reorganization with increased activation in the sensorimotor structures of the CON-H. True structural changes (e.g. axonal sprouting) do not have to be part of this type of reorganization. This explanation is supported by experiments in healthy subjects (Plewnia *et al.*, 2003) and studies in stroke patients (Liepert *et al.*, 2000; Shimizu *et al.*, 2002; Butefisch *et al.*, 2003) showing that reduced excitability in the M1 of one hemisphere is associated with disinhibition and enhanced excitability of the homologous M1, that this effect can occur immediately (Plewnia *et al.*, 2003), and that when it takes place in the intact M1 of stroke patients performance improvements are documented in the paretic hand (Mansur *et al.*, 2005).

The functional significance of coherence measures in the beta and alpha band of surface EEG or magnetoencephalography (MEG) has been well established (Classen *et al.*, 1998; Miltner *et al.*, 1999; Mima *et al.*, 2001*a*; Hummel and Gerloff, 2005). In the context of our comparative PET and TMS data and taking into account behavioural studies by others (Johansen-Berg *et al.*, 2002*a*), the present coherence results are likely to indicate that the observed activity of sensorimotor and premotor structures in the CON-H of stroke patients signifies integration into a functioning network, despite differences in impairment levels between our patients and those reported by Johansen-Berg.

Corticospinal connectivity

When stimulated with TMS, the M1 generates monosynaptic corticospinal commands, resulting in activation of alpha-motoneurons and finally in muscle responses (Asanuma, 1989; Goldring and Ratcheson, 1972). If the functional role of the (homologous area) iM1 were truly 'homologous', it should share this characteristic feature, i.e. stimulation of the iM1 (right hemisphere = CON-H) should result in MEPs in the recovered (right) hand. In none of the 11 patients, ipsilateral MEPs could be elicited. In contrast, stimulating the M1 of the DAM-H induced MEPs in the paretic hand. The only robust abnormality was an increased MT for M1 stimulation in the DAM-H indicating a persistent reduction in connectivity of the lesioned corticospinal tract. This result is in line with the recent observation of Werhahn *et al.* (2003) who demonstrated that single pulses of TMS given at 100 ms after the visual cue in a reaction time task were more effective in interfering with performance in stroke patients when applied to the M1 of the DAM-H than to the M1 of the CON-H.

Just because there are no ipsilateral MEPs, it cannot be concluded that the iM1 does not contribute to recovery. The functional role of uncrossed corticospinal pathways could become only 'unmasked' during voluntary action. Corticospinal connectivity during voluntary action can be assessed by computation of cortico–muscular coherence from EEG or MEG data. Mima *et al.* (2001*a*) have done this experiment in a group of stroke patients, and found no evidence for cortico–muscular coupling between CON-H and recovered hand during an isometric contraction task.

These physiological data are in line with anatomical studies performed by Kuypers and Lawrence showing that the uncrossed PT subserves only proximal and axial muscles—at least in the adult monkey (e.g. Lawrence and Kuypers, 1965; Kuypers, 1981).

Thus, if iM1 does not relay direct corticomotoneuronal connections, what role could it play in the recovery of function? A function such as mediating a simple reaction time movement is unlikely (Werhahn *et al.*, 2003). However, there is converging evidence that the M1 can process higher-order sensorimotor information such as direction selectivity, movement preparation, static or dynamic load effects (Alexander and Crutcher, 1990) or patterning of multijoint

activity (Ghez *et al.*, 1991; Martin and Ghez, 1993). Hocherman and Wise (1990, 1991) found a large population of trajectory-specific cells in the M1. Zhang *et al.* (1997) suggested that the M1 belongs to a distributed network such that its neuronal activity reflects the underlying network dynamics that translate a stimulus representation into a response representation. Results of two studies in which M1 was temporarily inactivated with repetitive TMS during motor sequence performance showed that both the contralateral and iM1 participate in coding of motor sequence complexity (Chen *et al.*, 1997; Gerloff *et al.*, 1998). Polysynaptic uncrossed (or double-crossed) connections from the iM1 to spinal alpha-motoneurons cannot be excluded on the basis of the available data, because the sensitivity of TMS and cortico–muscular coherence to those pathways has not been studied systematically.

The EEG coherence results may be taken as supportive evidence for the involvement of the ipsilateral BA 6 and BA 4 in higher-order motor processing, as they show enhanced connectivity of the contralesional central region with other motor and premotor areas in our patients. Similar enhancement of interregional coherences has been documented in healthy subjects in the initial phase of bimanual coordination learning (Andres *et al.*, 1999) and with increasing complexity of motor sequences (Manganotti *et al.*, 1998). That this can be seen in stroke patients during simple finger movement may be related to the fact that a simple movement carried out with a formerly paretic hand is more difficult. The relevance of the coherence data in this regard is further strengthened by the fact that M1 of the DAM-H in the patients appears less well connected to the other motor and premotor areas than in the control group. In an experiment on 11 patients with ischaemic lesions of various locations, Johansen-Berg *et al.* (2002*a*) applied single-pulse TMS to a point 2 cm anterior to the OP (approximately representing the contralesional PMd) and to another point 1 cm posterior to the OP, closer to the contralesional M1, in order to interfere with a finger movement. TMS applied to PMd early (100 ms) after the visual cue to move slowed reaction time by 12% compared with controls in patients with more prominent impairment. Stimulation 1-cm posterior to the OP produced no effect. This is in line with our findings suggesting the maximum of contralesional activation in BA 6 and the absence of a direct corticospinal projection from the contralesional M1. The functional relevance of the activation that we found in BA 6 of the DAM-H is supported by a recent paper of Fridman *et al.* (2004) who showed that TMS to this area was particularly effective in inducing delays in reaction time in the recovered hand of stroke patients with little impairment.

Concluding remarks and physiological considerations

The present data and recent behavioural experiments (Johansen-Berg *et al.*, 2002*a*; Werhahn *et al.*, 2003; Fridman *et al.*, 2004) indicate that both hemispheres contribute to recovery of function after capsular stroke, perhaps involved in differentiated aspects of motor planning and execution in patients with different degrees of impairment. It is very likely that restitution of near normal circuitry is the best basis for excellent recovery (Cramer, 2004). If perilesional, or in a wider sense, ipsilesional reorganization provides sufficient neural resources to compensate loss of function, good outcome seems to be most probable (Baron *et al.*, 2004). For these patients, also the notion that activity in the CON-H increases temporarily after the stroke but returns to baseline in the course of effective recovery (Ward *et al.*, 2003) is likely true. However, in many patients purely perilesional or ipsilesional reorganization might not be sufficient, and task-related increases of activity in the CON-H also persist in the chronic stage, as in our patients. On the basis of EMG monitoring during PET scanning and EEG recordings, it can be ruled out that activation of iM1 and premotor cortex of the CON-H is merely due to involuntary co-contractions of the healthy hand. Also, there was no evidence for bilateral proximal upper extremity synkinesias in our patients, and no comparable overactivation occurred in the M1 in the DAM-H, rendering this explanation unlikely. The relative importance of ipsilesional and contralesional BA 6 and BA 4 as well as of parietal areas, however, might differ substantially depending on the individual lesion pattern and other patient characteristics (Ward *et al.*, 2003; Luft *et al.*, 2004), and it would be consistent with our results and those of others that some aspects of activity in the CON-H interact with the DAM-H through interhemispheric inhibitory interactions (Murase *et al.*, 2004; Ward and Cohen, 2004).

The M1 and premotor cortex as well as the SPL of the CON-H showed increased activity after recovery from capsular infarction. Because all patients in our study had good recovery, it seems reasonable to propose that these contralesional structures, together with structures of the DAM-H such as the premotor cortex, are functioning parts of a reorganized cortical network and subserve motor recovery. This conclusion is supported by the cortico–cortical connectivity pattern as revealed by EEG coherence measurements and by the additional left cerebellar activation on PET. Considering our TMS and previous EEG–EMG coherence data (Mima *et al.*, 2001*b*), it is highly unlikely that in capsular stroke the contribution of the ipsilateral BA 4 (iM1) consists in the generation of an ipsilateral (uncrossed) monosynaptic corticospinal pathway. Thus, we favour the interpretation that the areas identified here are involved in higher-order motor processing such as selection, preparation, temporal or spatial organization of movement. This concept finds additional support in the EEG time-course data documenting that enhanced ipsilateral activity is present already before EMG onset.

In physiological terms, the present data are compatible with two interpretations: (i) effective recovery after stroke is based on repair mechanisms such as axonal sprouting with formation of new synapses and subsequently enhanced activation in novel parts of a neuronal network (for review see Chen *et al.*, 2001) or (ii) effective recovery can be achieved by enhanced

recruitment of pre-existing network elements, similar to the situation with complex movements compared to simple movements in the healthy brain (Sadato *et al.*, 1996; Manganotti *et al.*, 1998; Catalan *et al.*, 1999; Hummel *et al.*, 2003). The latter would mean that for stroke patients even the simplest movement is 'complex' and requires an extended network of premotor and sensorimotor structures. Both explanations are possible and, in our opinion, not mutually exclusive. Training-related structural changes in dendritic spine density and axonal connectivity have been shown in adult animals (Yuste and Bonhoeffer, 2001; Leuner *et al.*, 2003), and dynamic reorganization in the course of learning a complex motor task is also a well-documented phenomenon (Karni *et al.*, 1995; Andres *et al.*, 1999). Hence, it is likely that in the course of recovery, a post-stroke brain undergoes some structural change. For example, neuronal excitability and long-term potentiation are enhanced after experimental brain lesions (Hagemann *et al.*, 1998) and provide a basis for functional and structural adaptive changes. In this connection, it is worth noting that in some stroke patients the M1 of the CON-H is disinhibited (Liepert *et al.*, 2000). Given the link between enhanced excitability and plasticity (Ziemann *et al.*, 2001; Stefan *et al.*, 2002; Plewnia *et al.*, 2004), this might allow for a more effective adaptation. Clinical experience suggests that for the majority of recovered stroke patients any movement with the formerly paretic limb is more challenging than before the stroke. This aspect would then correspond to the upregulation of activity in pre-existing parts of the motor network such as contralesional BA 6 and BA 4, SPL and corresponding aspects of the cerebellum (Baron *et al.*, 2004). If upregulation were the only mechanism, we would expect concomitant upregulation of all corresponding areas in the DAM-H as well. As this is not the case (the overall activation pattern changes), a combination of 'true' plastic changes and recruitment of pre-existing resources appears to be more likely. Although there seems to be a plethora of ways for cortical assemblies to compute a movement and use alternative routes to generate corticospinal control (Dobkin, 2003), an effective and lasting recruitment of uncrossed corticospinal tract fibres as seen with very early lesions, e.g. perinatal periventricular lesions (Staudt *et al.*, 2002; Gerloff *et al.*, 2005) does not appear to be a relevant mechanism of recovery in adult stroke patients. On the contrary, converging evidence points to a crucial contribution of non-primary motor areas of both hemispheres, in particular BA 6 (Johansen-Berg *et al.*, 2002*b*; Fridman *et al.*, 2004), but according to our PET data also the SPL. Finally, our data in well-recovered patients do not preclude a more active role of ipsilateral projections from the intact M1 early after a stroke (Marshall *et al.*, 2000; Ward *et al.*, 2003) or in patients with larger lesions, greater neurological deficit and less successful recovery (Turton *et al.*, 1996; Carey *et al.*, 2002; Butefisch *et al.*, 2003). Effective recovery may be associated with a dynamic change from initially excessive activation in the CON-H toward a more lateralized pattern in the chronic stage, more similar to healthy subjects (Cramer, 2004; Rossini *et al.*, 2003; Traversa *et al.*, 2000; Ward *et al.*, 2003). Of note, there is some persistent enhancement of activation in contralesional motor areas which is likely to be involved in the control of recovered hand function.

With respect to therapeutic interventions geared at modulating cortical activity in order to facilitate recovery after stroke or reading out meaningful neuronal signals for improving motor functions by neuroprosthetic devices, the present data suggest that enhancing activity in BA 4 of the DAM-H (Hummel *et al.*, 2005) and also BA 6 and SPL of the CON-H are interesting targets. Also decreasing activity in the intact M1 (CON-H) appears to contribute to motor improvements in the paretic hand. Neurostimulation or electrode placement in areas of the CON-H has the obvious advantage that excitatory electrical currents or mechanical irritations are not applied directly to damaged or perilesional tissue. Also with respect to potential side effects (e.g. seizure induction), manipulation of non-primary motor areas is likely to be safer than targeting M1 directly.

Acknowledgements

We are grateful to Ms S. Thomas, laboratory technician, for technical support, and to D.G. Schoenberg, MSc, for skillful editing. The study was supported by NIH intramural, C.G. and A.S. by grants of the Deutsche Forschungsgemeinschaft (Ge 844, SFB 307/B12, SFB 550/C5).

References

Ago T, Kitazono T, Ooboshi H, Takada J, Yoshiura T, Mihara F, et al. Deterioration of pre-existing hemiparesis brought about by subsequent ipsilateral lacunar infarction. J Neurol Neurosurg Psychiatry 2003; 74: 1152–3.

Alexander GE, Crutcher MD. Neural representations of the target (goal) of visually guided arm movements in three motor areas of the monkey. J Neurophysiol 1990; 64: 164–78.

Amjad AM, Halliday DM, Rosenberg JR, Conway BA. An extended difference of coherence test for comparing and combining several independent coherence estimates: theory and application to the study of motor units and physiological tremor. J Neurosci Methods 1997; 73: 69–79.

Andres FG, Mima T, Schulman AE, Dichgans J, Hallett M, Gerloff C. Functional coupling of human cortical sensorimotor areas during bimanual skill acquisition. Brain 1999; 122: 855–70.

Asanuma H. The Motor Cortex. New York: Raven Press, 1989.

Baron JC, Cohen LG, Cramer SC, Dobkin BH, Johansen-Berg H, Loubinoux I, et al. Neuroimaging in stroke recovery: a position paper from the First International Workshop on Neuroimaging and Stroke Recovery. Cerebrovasc Dis 2004; 18: 260–7.

Braak H. The pigment architecture of the human frontal lobe. I. Precentral, subcentral and frontal region. Anat Embryol (Berl) 1979; 157: 35–68.

Brown JA, Lutsep H, Cramer SC, Weinand M. Motor cortex stimulation for enhancement of recovery after stroke: case report. Neurol Res 2003; 25: 815–8.

Butefisch CM, Netz J, Wessling M, Seitz RJ, Homberg V. Remote changes in cortical excitability after stroke. Brain 2003; 126: 470–81.

Calautti C, Baron JC. Functional neuroimaging studies of motor recovery after stroke in adults: a review. Stroke 2003; 34: 1553–66.

Calautti C, Leroy F, Guincestre JY, Baron JC. Dynamics of motor network overactivation after striatocapsular stroke: a longitudinal PET study using a fixed-performance paradigm. Stroke 2001; 32: 2534–42.

Caminiti R, Ferraina S, Mayer AB. Visuomotor transformations: early cortical mechanisms of reaching. Curr Opin Neurobiol 1998; 8: 753–61.

Cao Y, D'Olhaberriague L, Vikingstad EM, Levine SR, Welch KM. Pilot study of functional MRI to assess cerebral activation of motor function after poststroke hemiparesis. Stroke 1998; 29: 112–22.

Carey JR, Kimberley TJ, Lewis SM, Auerbach EJ, Dorsey L, Rundquist P, et al. Analysis of fMRI and finger tracking training in subjects with chronic stroke. Brain 2002; 125: 773–88.

Catalan MJ, Honda M, Weeks RA, Cohen LG, Hallett M. The functional neuroanatomy of simple and complex sequential finger movements: a PET study. Brain 1998; 121: 253–64.

Catalan MJ, Ishii K, Honda M, Samii A, Hallett M. A PET study of sequential finger movements of varying length in patients with Parkinson's disease. Brain 1999; 122: 483–95.

Chen R, Gerloff C, Hallett M, Cohen LG. Involvement of the ipsilateral motor cortex in finger movements of different complexities. Ann Neurol 1997; 41: 247–54.

Chen R, Garg RR, Lozano AM, Lang AE. Effects of internal globus pallidus stimulation on motor cortex excitability. Neurology 2001; 56: 716–23.

Chen Y, Ding M, Kelso JA. Task-related power and coherence changes in neuromagnetic activity during visuomotor coordination. Exp Brain Res 2003; 148: 105–16.

Chollet F, DiPiero V, Wise RJ, Brooks DJ, Dolan RJ, Frackowiak RS. The functional anatomy of motor recovery after stroke in humans: a study with positron emission tomography. Ann Neurol 1991; 29: 63–71.

Classen J, Gerloff C, Honda M, Hallett M. Integrative visuomotor behavior is associated with interregionally coherent oscillations in the human brain. J Neurophysiol 1998; 79: 1567–73.

Conway BA, Halliday DM, Farmer SF, Shahani U, Maas P, Weir AI, et al. Synchronization between motor cortex and spinal motoneuronal pool during the performance of a maintained motor task in man. J Physiol (Lond) 1995; 489: 917–24.

Cramer SC. Functional magnetic resonance imaging in stroke recovery. Phys Med Rehabil Clin N Am 2003; 14: S47–55.

Cramer SC. Functional imaging in stroke recovery. Stroke 2004; 35: 2695–8.

Cramer SC, Nelles G, Benson RR, Kaplan JD, Parker RA, Kwong KK, et al. A functional MRI study of subjects recovered from hemiparetic stroke. Stroke 1997; 28: 2518–27.

Cramer SC, Nelles G, Schaechter JD, Kaplan JD, Finklestein SP, Rosen BR. A functional MRI study of three motor tasks in the evaluation of stroke recovery. Neurorehabil Neural Repair 2001; 15: 1–8.

Dettmers C, Young A, Rommel T, Hartmann A, Weingart O, Baron JC. CO2 reactivity in the ischaemic core, penumbra, and normal tissue 6 hours after acute MCA-occlusion in primates. Acta Neurochir 1993; 125: 150–5.

Dobkin BH. Functional MRI: a potential physiologic indicator for stroke rehabilitation interventions. Stroke 2003; 34: e23–8.

Fein G, Raz J, Brown FF, Merrin EL. Common reference coherence data are confounded by power and phase effects. Electroencephalogr Clin Neurophysiol 1988; 69: 581–4.

Feydy A, Carlier R, Roby-Brami A, Bussel B, Cazalis F, Pierot L, et al. Longitudinal study of motor recovery after stroke: recruitment and focusing of brain activation. Stroke 2002; 33: 1610–7.

Fisher CM. Concerning the mechanism of recovery in stroke hemiplegia. Can J Neurol Sci 1992; 19: 57–63.

Fridman EA, Hanakawa T, Chung M, Hummel F, Leiguarda RC, Cohen LG. Reorganization of the human ipsilesional premotor cortex after stroke. Brain 2004; 127: 747–58.

Friehs GM, Zerris VA, Ojakangas CL, Fellows MR, Donoghue JP. Brain-machine and brain-computer interfaces. Stroke 2004; 35: 2702–5.

Friston KJ, Holmes AP, Worsley KJ. How many subjects constitute a study? Neuroimage 1999; 10: 1–5.

Fujii Y, Nakada T. Cortical reorganization in patients with subcortical hemiparesis: neural mechanisms of functional recovery and prognostic implication. J Neurosurg 2003; 98: 64–73.

Gerloff C, Hadley J, Richard J, Uenishi N, Honda M, Hallett M. Functional coupling and regional activation of human cortical motor areas during simple, internally paced and externally paced finger movements. Brain 1998; 121: 1513–31.

Gerloff C, Braun C, Hallett M. Coherence, cortico-cortical. In: Hallett M, editor. Movement disorders (handbook of neurophysiology). Vol 1. Amsterdam: Elsevier, 2003. p. 77–85.

Gerloff C, Braun C, Staudt M, Li Hegner Y, Dichgans J, Krägeloh-Mann I. Coherent corticomuscular oscillations originate from primary motor cortex: Evidence from patients with early brain lesions. Hum Brain Mapp 2005, in press.

Geyer S, Matelli M, Luppino G, Zilles K. Functional neuroanatomy of the primate isocortical motor system. Anat Embryol (Berl) 2000; 202: 443–74.

Ghez C, Hening W, Gordon J. Organization of voluntary movement. Curr Opin Neurobiol 1991; 1: 664–71.

Goldring S, Ratcheson R. Human motor cortex: sensory input data from single neuron recordings. Science 1972; 175: 1493–5.

Gould HJ, Cusick CG, Pons TP, Kaas JH. The relationship of corpus callosum connections to electrical stimulation maps of motor, supplementary motor, and the frontal eye fields in owl monkeys. J Comp Neurol 1986; 247: 297–325.

Green JB, Bialy Y, Sora E, Ricamato A. High-resolution EEG in poststroke hemiparesis can identify ipsilateral generators during motor tasks. Stroke 1999; 30: 2659–65.

Hagemann G, Redecker C, Neumann-Haefelin T, Freund HJ, Witte OW. Increased long-term potentiation in the surround of experimentally induced focal cortical infarction. Ann Neurol 1998; 44: 255–8.

Hamdy S, Rothwell JC. Gut feelings about recovery after stroke: the organization and reorganization of human swallowing motor cortex. Trends Neurosci 1998; 21: 278–82.

Hebb DO. The organization of behavior: A neurophysiological theory. New York: Wiley, 1949.

Herscovitch P, Markham J, Raichle ME. Brain blood flow measured with intravenous H2(15)O. I. Theory and error analysis. J Nucl Med 1983; 24: 782–9.

Hocherman S, Wise SP. Trajectory-selective neuronal activity in the motor cortex of rhesus monkeys (Macaca mulatta). Behav Neurosci 1990; 104: 495–9.

Hocherman S, Wise SP. Effects of hand movement path on motor cortical activity in awake, behaving rhesus monkeys. Exp Brain Res 1991; 83: 285–302.

Hummel F, Gerloff C. Larger interregional synchrony is associated with greater behavioral success in a complex sensory integration task in humans. Cereb Cortex 2005; 15: 670–8.

Hummel F, Kirsammer R, Gerloff C. Ipsilateral cortical activation during finger sequences of increasing complexity: representation of movement difficulty or memory load? Clin Neurophysiol 2003; 114: 605–13.

Hummel F, Celnik P, Giraux P, Floel A, Wu WH, Gerloff C, et al. Effects of non-invasive cortical stimulation on skilled motor function in chronic stroke. Brain 2005; 128: 490–9.

Johansen-Berg H, Dawes H, Guy C, Smith SM, Wade DT, Matthews PM. Correlation between motor improvements and altered fMRI activity after rehabilitative therapy. Brain 2002a; 125: 2731–42.

Johansen-Berg H, Rushworth MF, Bogdanovic MD, Kischka U, Wimalaratna S, Matthews PM. The role of ipsilateral premotor cortex in hand movement after stroke. Proc Natl Acad Sci USA 2002b; 99: 14518–23.

Karbe H, Thiel A, Weber-Luxenburger G, Herholz K, Kessler J, Heiss WD. Brain plasticity in poststroke aphasia: what is the contribution of the right hemisphere? Brain Lang. 1998; 64: 215–30.

Karni A, Meyer G, Jezzard P, Adams MM, Turner R, Ungerleider LG. Functional MRI evidence for adult motor cortex plasticity during motor skill learning. Nature 1995; 377: 155–58.

Kennedy PR, Kirby MT, Moore MM, King B, Mallory A. Computer control using human intracortical local field potentials. IEEE Trans Neural Syst Rehabil Eng 2004; 12: 339–44.

Kobayashi M, Ng J, Theoret H, Pascual-Leone A. Modulation of intracortical neuronal circuits in human hand motor area by digit stimulation. Exp Brain Res 2003; 149: 1–8.

Kuypers HG. Anatomy of the descending pathways. In: Brooks VB, editor. Handbook of physiology, section 1: the nervous system. Vol II. Motor control. Bethesda: American Physiological Society; 1981. p. 597–666.

Lawrence DG, Kuypers HG. Pyramidal and non-pyramidal pathways in monkeys: anatomical and functional correlation. Science 1965; 148: 973–5.

Leuner B, Falduto J, Shors TJ. Associative memory formation increases the observation of dendritic spines in the hippocampus. J Neurosci 2003; 23: 659–65.

Liepert J, Terborg C, Weiller C. Motor plasticity induced by synchronized thumb and foot movements. Exp Brain Res 1999; 125: 435–9.

Liepert J, Hamzei F, Weiller C. Motor cortex disinhibition of the unaffected hemisphere after acute stroke. Muscle Nerve 2000; 23: 1761–3.

Luft AR, Waller S, Forrester L, Smith GV, Whitall J, Macko RF, et al. Lesion location alters brain activation in chronically impaired stroke survivors. Neuroimage 2004; 21: 924–35.

Manganotti P, Gerloff C, Toro C, Katsuta H, Sadato N, Zhuang P, et al. Task-related coherence and task-related spectral power changes during sequential finger movements. Electroencephalogr Clin Neurophysiol 1998; 109: 50–62.

Mansur CG, Fregni F, Boggio PS, Riberto M, Gallucci-Neto J, Santos CM, et al. A sham stimulation-controlled trial of rTMS of the unaffected hemisphere in stroke patients. Neurology 2005; 64: 1802–4.

Marshall RS, Perera GM, Lazar RM, Krakauer JW, Constantine RC, DeLaPaz RL. Evolution of cortical activation during recovery from corticospinal tract infarction. Stroke 2000; 31: 656–61.

Martin JH, Ghez C. Differential impairments in reaching and grasping produced by local inactivation within the forelimb representation of the motor cortex in the cat. Exp Brain Res 1993; 94: 429–43.

Martin PI, Naeser MA, Theoret H, Tormos JM, Nicholas M, Kurland J, et al. Transcranial magnetic stimulation as a complementary treatment for aphasia. Semin Speech Lang 2004; 25: 181–91.

Merzenich MM, Jenkins WM. Reorganization of cortical representations of the hand following alterations of skin inputs induced by nerve injury, skin island transfers, and experience. J Hand Ther 1993; 6: 89–104.

Miltner WH, Braun C, Arnold M, Witte H, Taub E. Coherence of gamma-band EEG activity as a basis for associative learning. Nature 1999; 397: 434–6.

Mima T, Steger J, Schulman AE, Gerloff C, Hallett M. Electroencephalographic measurement of motor cortex control of muscle activity in humans. Clin Neurophysiol 2000; 111: 326–37.

Mima T, Matsuoka T, Hallett M. Information flow from the sensorimotor cortex to muscle in humans. Clin Neurophysiol 2001a; 112: 122–6.

Mima T, Toma K, Koshy B, Hallett M. Coherence between cortical and muscular activities after subcortical stroke. Stroke 2001b; 32: 2597–601.

Murase N, Duque J, Mazzocchio R, Cohen LG. Influence of interhemispheric interactions on motor function in chronic stroke. Ann Neurol 2004; 55: 400–9.

Nelles G, Spiekermann G, Jueptner M, Leonhardt G, Muller S, Gerhard H, et al. Reorganization of sensory and motor systems in hemiplegic stroke patients. A positron emission tomography study. Stroke 1999; 30: 1510–6.

Netz J, Lammers T, Homberg V. Reorganization of motor output in the non-affected hemisphere after stroke. Brain 1997; 120: 1579–86.

Nudo RJ. Functional and structural plasticity in motor cortex: implications for stroke recovery. Phys Med Rehabil Clin N Am 2003; 14: S57–76.

Nudo RJ, Wise BM, SiFuentes F, Milliken GW. Neural substrates for the effects of rehabilitative training on motor recovery after ischemic infarct. Science 1996; 272: 1791–4.

Pariente J, Loubinoux I, Carel C, Albucher JF, Leger A, Manelfe C, et al. Fluoxetine modulates motor performance and cerebral activation of patients recovering from stroke. Ann Neurol 2001; 50: 718–29.

Pfurtscheller G, Andrew C. Event-Related changes of band power and coherence: methodology and interpretation. J Clin Neurophysiol 1999; 16: 512–9.

Pfurtscheller G, Aranibar A. Event-related cortical desynchronization detected by power measurements of scalp EEG. Electroencephalogr Clin Neurophysiol 1977; 42: 817–26.

Pfurtscheller G, Graimann B, Huggins JE, Levine SP, Schuh LA. Spatiotemporal patterns of beta desynchronization and gamma synchronization in corticographic data during self-paced movement. Clin Neurophysiol 2003; 114: 1226–36.

Pfurtscheller G, Stancak A Jr, Edlinger G. On the existence of different types of central beta rhythms below 30 Hz. Electroencephalogr Clin Neurophysiol 1997; 102: 316–25.

Pineiro R, Pendlebury S, Johansen-Berg H, Matthews PM. Altered hemodynamic responses in patients after subcortical stroke measured by functional MRI. Stroke 2002; 33: 103–9.

Plewnia C, Lotze M, Gerloff C. Disinhibition of the contralateral motor cortex by low-frequency rTMS. Neuroreport 2003; 14: 609–12.

Plewnia C, Hoppe J, Cohen LG, Gerloff C. Improved motor skill acquisition after selective stimulation of central norepinephrine. Neurology 2004; 62: 2124–6.

Poline JB, Worsley KJ, Evans AC, Friston KJ. Combining spatial extent and peak intensity to test for activations in functional imaging. Neuroimage 1997; 5: 83–96.

Rappelsberger P, Petsche H. Probability mapping: power and coherence analyses of cognitive processes. Brain Topogr 1988; 1: 46–54.

Rossini PM, Dal Forno G. Integrated technology for evaluation of brain function and neural plasticity. Phys Med Rehabil Clin N Am 2004; 15: 263–306.

Rossini PM, Calautti C, Pauri F, Baron JC. Post-stroke plastic reorganisation in the adult brain. Lancet Neurol 2003; 2: 493–502.

Rouiller EM, Babalian A, Kazennikov O, Moret V, Yu XH, Wiesendanger M. Transcallosal connections of the distal forelimb representations of the primary and supplementary motor cortical areas in macaque monkeys. Exp Brain Res 1994; 102: 227–43.

Sadato N, Campbell G, Ibanez V, Deiber MP, Hallett M. Complexity affects regional cerebral blood flow change during sequential finger movements. J Neurosci 1996; 16: 2691–700.

Sailer A, Dichgans J, Gerloff C. The influence of normal aging on the cortical processing of a simple motor task. Neurology 2000; 55: 979–85.

Seitz RJ, Hoflich P, Binkofski F, Tellmann L, Herzog H, Freund HJ. Role of the premotor cortex in recovery from middle cerebral artery infarction. Arch Neurol 1998; 55: 1081–8.

Sette G, Baron JC, Mazoyer B, Levasseur M, Pappata S, Crouzel C. Local brain haemodynamics and oxygen metabolism in cerebrovascular disease. Positron emission tomography. Brain 1989; 112: 931–51.

Shaw JC. Correlation and coherence analysis of the EEG: a selective tutorial review. Int J Psychophysiol 1984; 1: 255–66.

Shimizu T, Hosaki A, Hino T, Sato M, Komori T, Hirai S, et al. Motor cortical disinhibition in the unaffected hemisphere after unilateral cortical stroke. Brain 2002; 125: 1896–907.

Staudt M, Grodd W, Gerloff C, Erb M, Stitz J, Krageloh-Mann I. Two types of ipsilateral reorganization in congenital hemiparesis: a TMS and fMRI study. Brain 2002; 125: 2222–37.

Stefan K, Kunesch E, Benecke R, Cohen LG, Classen J. Mechanisms of enhancement of human motor cortex excitability induced by interventional paired associative stimulation. J Physiol 2002; 543: 699–708.

Tanaka Y, Yoshida A, Kawahata N, Hashimoto R, Obayashi T. Diagonistic dyspraxia. Clinical characteristics, responsible lesion and possible underlying mechanism. Brain 1996; 119: 859–73.

Thompson ML, Thickbroom GW, Laing B, Wilson S, Mastaglia FL. Changes in the organisation of the corticomotor projection to the hand after subcortical stroke. Electroencephalogr Clin Neurophysiol 1995; 97: S191.

Traversa R, Cicinelli P, Oliveri M, Giuseppina Palmieri M, Filippi MM, Pasqualetti P, et al. Neurophysiological follow-up of motor cortical output in stroke patients. Clin Neurophysiol 2000; 111: 1695–703.

Turton A, Wroe S, Trepte N, Fraser C, Lemon RN. Contralateral and ipsilateral EMG responses to transcranial magnetic stimulation during recovery of arm and hand function after stroke. Electroencephalogr Clin Neurophysiol 1996; 101: 316–28.

Verleger R, Adam S, Rose M, Vollmer C, Wauschkuhn B, Kompf D. Control of hand movements after striatocapsular stroke: high-resolution temporal

analysis of the function of ipsilateral activation. Clin Neurophysiol 2003; 114: 1468–76.

Wang XQ, Merzenich MM, Sameshima K, Jenkins WM. Remodeling of hand representation in adult cortex determined by timing of tactile stimulation. Nature 1995; 378: 71–5.

Ward NS, Brown MM, Thompson AJ, Frackowiak RS. Neural correlates of outcome after stroke: a cross-sectional fMRI study. Brain 2003; 126: 1430–48.

Ward NS, Cohen LG. Mechanisms underlying recovery of motor function after stroke. Arch Neurol 2004; 61: 1844–8.

Wassermann EM, Pascual-Leone A, Hallett M. Cortical motor representation of the ipsilateral hand and arm. Exp Brain Res 1994; 100: 121–32.

Weiller C, Chollet F, Friston KJ, Wise RJ, Frackowiak RSJ. Functional reorganization of the brain in recovery from striatocapsular infarction in man. Ann Neurol 1992; 31: 463–72.

Weiller C, Ramsay SC, Wise RJ, Friston KJ, Frackowiak RSJ. Individual patterns of functional reorganization in the human cerebral cortex after capsular infarction. Ann Neurol 1993; 33: 181–9.

Weiller C, Isensee C, Rijntjes M, Huber W, Muller S, Bier D, et al. Recovery from Wernicke's aphasia: a positron emission tomographic study. Ann Neurol 1995; 37: 723–32.

Werhahn KJ, Conforto AB, Kadom N, Hallett M, Cohen LG. Contribution of the ipsilateral motor cortex to recovery after chronic stroke. Ann Neurol 2003; 54: 464–72.

Wessberg J, Stambaugh CR, Kralik JD, Beck PD, Laubach M, Chapin JK, et al. Real-time prediction of hand trajectory by ensembles of cortical neurons in primates. Nature 2000; 408: 361–5.

Wexler BE, Fulbright RK, Lacadie CM, Skudlarski P, Kelz MB, Constable RT, et al. An fMRI study of the human cortical motor system response to increasing functional demands. Magn Reson Imaging 1997; 15: 385–96.

White LE, Andrews TJ, Hulette C, Richards A, Groelle M, Paydarfar J, et al. Structure of the human sensorimotor system. I: Morphology and cytoarchitecture of the central sulcus. Cereb Cortex 1997; 7: 18–30.

Winhuisen L, Thiel A, Schumacher B, Kessler J, Rudolf J, Haupt WF, et al. Role of the contralateral inferior frontal gyrus in recovery of language function in poststroke aphasia. A combined repetitive transcranial magnetic stimulation and positron emission tomography study. Stroke 2005; 36: 1759–63.

Wise SP. The primate premotor cortex: past, present, and preparatory. Annu Rev Neurosci 1985; 8: 1–19.

Wise SP, Boussaoud D, Johnson PB, Caminiti R. Premotor and parietal cortex: corticocortical connectivity and combinatorial computations. Annu Rev Neurosci 1997; 20: 25–42.

Wittenberg GF, Bastian AJ, Dromerick AW, Thach WT, Powers WJ. Mirror movements complicate interpretation of cerebral activation changes during recovery from subcortical infarction. Neurorehabil Neural Repair 2000; 14: 213–21.

Wolpaw JR, Birbaumer N, McFarland DJ, Pfurtscheller G, Vaughan TM. Brain-computer interfaces for communication and control. Clin Neurophysiol 2002; 113: 767–91.

Woods RP. Modeling for intergroup comparisons of imaging data. Neuroimage 1996; 4: S84–94.

Xerri C, Merzenich MM, Peterson BE, Jenkins W. Plasticity of primary somatosensory cortex paralleling sensorimotor skill recovery from stroke in adult monkeys. J Neurophysiol 1998; 79: 2119–48.

Yuste R, Bonhoeffer T. Morphological changes in dendritic spines associated with long-term synaptic plasticity. Annu Rev Neurosci 2001; 24: 1071–89.

Zhang J, Riehle A, Requin J, Kornblum S. Dynamics of single neuron activity in monkey primary motor cortex related to sensorimotor transformation. J Neurosci 1997; 17: 2227–46.

Ziemann U, Ishii K, Borgheresi A, Yaseen Z, Battaglia F, Hallett M, et al. Dissociation of the pathways mediating ipsilateral and contralateral motor-evoked potentials in human hand and arm muscles. J Physiol 1999; 518 : 895–906.

Ziemann U, Muellbacher W, Hallett M, Cohen LG. Modulation of practice-dependent plasticity in human motor cortex. Brain 2001; 124: 1171–81.

Journal of Cerebral Blood Flow & Metabolism (2006) 26, 291–300

www.jcbfm.com

Quantitative evaluation of cerebral hemodynamics in patients with moyamoya disease by dynamic susceptibility contrast magnetic resonance imaging—comparison with positron emission tomography

Yoji Tanaka[1], Tadashi Nariai[1], Tsukasa Nagaoka[1,2], Hideaki Akimoto[1,3], Kiichi Ishiwata[4], Kenji Ishii[4], Yoshiharu Matsushima[1] and Kikuo Ohno[1]

[1]*Department of Neurosurgery, Graduate School, Tokyo Medical and Dental University, Tokyo, Japan;* [2]*Department of Physiology and Biophysics, Albert Einstein College of Medicine, New York, New York, USA;* [3]*Department of Neurosurgery, Musashino Red Cross Hospital, Musashino, Japan;* [4]*Positron Medical Center, Tokyo Metropolitan Institute of Gerontology, Tokyo, Japan*

We examined whether the degree of hemodynamic stress in patients with chronic occlusive cerebral vascular disease can be quantitatively evaluated with the use of perfusion-weighted magnetic resonance imaging (PWI). Thirty-six patients with moyamoya disease (mean age, 26.8 years; range, 18 to 59) underwent PWI and positron emission tomography (PET) within a month's interval. The PWI data were calculated by three different analytic methods. The cerebral blood flow (CBF) ratio, cerebral blood volume (CBV) ratio, and mean transit time (MTT) of the anterior circulation were calculated using the cerebellum as a control region and compared with PET data on the same three parameters and oxygen extraction fraction (OEF). Parametric maps of PWI attained a higher resolution than the PET maps and revealed focal perfusion failure on a gyrus-by-gyrus level. The relative CBV and MTT obtained with PWI showed significant linear correlations with the corresponding PET values (CBV, $R^2 = 0.47$ to 0.58; MTT, $R^2 = 0.32$ to 0.68). We also found that we could detect regions with abnormally elevated OEF and CBV based on the delay of PWI-measured MTT relative to the control region by defining a 2.0-sec delay as a threshold. The sensitivity and specificity were 92.3% and 100% in detecting regions with abnormally elevated OEF, and 20.0% and 100% in detecting regions with abnormally elevated CBV, respectively. Among the parameters obtained with PWI, our results suggested that the relative CBV value and delay of MTT might be quantitatively manipulated to assist in clinical decision-making for patients with moyamoya disease.
Journal of Cerebral Blood Flow & Metabolism (2006) **26,** 291–300. doi:10.1038/sj.jcbfm.9600187; published online 27 July 2005

Keywords: blood volume; cerebral blood flow; misery perfusion; oxygen extraction fraction; transit time

Introduction

To understand the pathophysiology and determine the optimal treatment of occlusive cerebrovascular disease, it is vital to clarify the degree of hemodynamic compromise in each patient. Patients at a high risk of ischemic stroke generally exhibit abnormally high oxygen extraction fraction (OEF) and elevated cerebral blood volume (CBV), a combination of states described as misery perfusion or grade 2 hemodynamic stress (Derdeyn *et al,* 2002; Grubb *et al,* 1998). The concurrent measurement of cerebral blood flow (CBF), metabolism, and blood volume on the same occasion by positron emission tomography (PET) serves as the optimal method for evaluating hemodynamics in patients. Positron emission tomography is usually unavailable in daily clinical practice, however, and it provides only poor information on the structural integrity of hypoperfused tissue.

Perfusion-weighted magnetic resonance (MR) imaging (MRI) (PWI) provides various parameters

Correspondence: Dr Tadashi Nariai, Department of Neurosurgery, Tokyo Medical and Dental University, 1-5-45 Yushima, Bunkyo-ku, Tokyo 113, Japan. E-mail: nariai.nsrg@tmd.ac.jp
Received 1 February 2005; revised 13 May 2005; accepted 21 June 2005; published online 27 July 2005

of cerebral dynamics noninvasively and in less time than PET. A newly developed technique for determining absolute CBF using MRI by introducing an empirical normalization constant in animals (Ostergaard *et al*, 1998*b*) and humans (Ostergaard *et al*, 1998*a*) has recently been applied to evaluate occlusive cerebrovascular disorder (Baird and Warach, 1998; Maeda *et al*, 1999; Warach *et al*, 1996). To apply this technique effectively in decision-making for individual patients, however, we first have to clarify the reliability of the obtained parameters. In this study, we examined the same individual patients by PWI and PET within a short period in an attempt to confirm whether the numerical parameters obtained with PWI can be manipulated as quantitative values.

Moyamoya disease is a slowly progressive cerebrovascular disease with terminal internal carotid artery (ICA) occlusion and collateral formation of abnormal arteries (Matsushima, 1999; Suzuki and Takaku, 1969). Patients with moyamoya disease show various degrees of hemodynamic insufficiency and clinical symptoms. This variability might be due to the variable interaction between the worsening hemodynamic factors with disease progression and the protection conferred by the collateral development (Ikezaki *et al*, 1994; Nariai *et al*, 2005). The ischemic episodes in moyamoya patients are often caused by hemodynamic stress rather than thromboembolism (Ikezaki *et al*, 1994). These features of moyamoya disease make it an appropriate subject for comparing quantified hemodynamic factors with multiple modalities (Nariai *et al*, 1995). The use of PWI in moyamoya patients has been reported by several groups (Calamante *et al*, 2001; Kassner *et al*, 2003; Lee *et al*, 2003; Tsuchiya *et al*, 1998; Yamada *et al*, 1999). However, the accuracy of quantitative evaluation of cerebral hemodynamics by PWI in moyamoya patients has not yet been discussed. Moreover, we have yet to understand the significance of the abnormalities in the PWI parameters in relation to the severity of hemodynamics in patients with occlusive cerebrovascular disease. The purposes of the present study were to evaluate whether PWI can accurately measure hemodynamic parameters, and to certify the reliability of quantitation. We also discussed the range of application of this method in various types of cerebrovascular disease.

Subjects and methods

Forty-one examinations of 36 patients with angiographically confirmed moyamoya disease were evaluated in this study. The subjects consisted of 4 men and 32 women, ranging in age from 18 to 59 years (mean age, 26.8 years). All of the patients exhibited complete obstruction or stenosis in the terminal portion of bilateral ICA with moyamoya vessels, but no abnormal findings in cerebellar circulation. They underwent both PWI scan and PET scan within the same 30-day period for diagnosis or follow-up evaluation of cerebral hemodynamics. Five of the patients underwent postoperative scans at least 1 year after the bilateral indirect bypass surgery (encephalo-duro-arterio-synangiosis). The transient ischemic symptoms disappeared and good revascularization was confirmed by angiography in all five of these patients at the time of the scanning. Thus, their hemodynamic status was confirmed to be stable when the comparative examinations using PWI and PET were performed.

Perfusion-Weighted Magnetic Resonance Imaging

The MR imaging studies were performed using a 1.5-T superconducting system with a 25 mT/m maximal gradient capacity (Magnetom Vision; Siemens, Erlangen, Germany) and a circularly polarized head coil. Perfusion-weighted magnetic resonance imaging was performed using a multislice, single-shot, spin-echo echo-planar imaging sequence. The imaging parameters were as follows: repetition time = 1200 ms, echo time = 66 ms, field of view = 230×230 mm^2, matrix size = 128×128. A total of 50 scans with 7 slices were repeated in quick succession without delay (3 scans before injection). The device scanned a series of seven 5-mm-thick slices separated by 7.5-mm gaps. The lowermost slice included the cerebellar hemisphere as a control area, and another slice included the ICA to enable estimation of the arterial input function (AIF). The seven slices were also set to cover both cerebral hemispheres. Each patient received a bolus injection of gadodiamide (0.2 mmol/kg body weight; OMNISCAN, Daiichi Seiyaku, Tokyo, Japan) via an antecubital vein using a power injector (Nemoto Kyorindo, Japan) at a rate of 3 mL/sec, followed by a 15-mL saline flush.

Perfusion-Weighted Magnetic Resonance Imaging Image Processing

All of the PWI data and PET data were transferred to a personal computer after the measurement. The PWI data were analyzed by three separate analyses using Dr View/LINUX R2.0 software (Asahi Kasei Information Systems, Tokyo, Japan). In preparation, we calculated the transverse relaxation rate (ΔR_2) by the equation $\Delta R_2(t) = -\ln(S(t)/S0)/TE$, where $S(t)$ was signal intensity at time t, $S0$ was the precontrast baseline signal intensity, and TE was the sequence echo time. Next, we applied a 3×3 uniform smoothing kernel to the raw image and commenced the three analyses to generate the parameters. In the first analysis, we generated a CBF map and CBV map by deconvolving the change in tissue concentration over the first pass of contrast agent with an arterial AIF using singular value decomposition (SVD) (Ostergaard *et al*, 1996*a*, *b*) (deconvolution method) and then calculating the mean transit time (MTT) by CBV/CBF. While this method generally yields accurate measurements of CBF, the flow estimates using SVD are susceptible to error due to bolus delay and dispersion. To improve reliability, we evaluated the PWI data by our second analysis, a pixel-based

numerical integration analysis with the measured data for calculation of the relative CBV (*rCBV*) and relative MTT (*rMTT*) (PIX method). The *rCBV* and *rMTT* were directly calculated from the time–ΔR_2 curve

$$rCBV = \int_{T_{start}}^{T_{end}} dt \cdot \Delta R_2(t) \quad (1)$$

$$rMTT = \frac{\int_{T_{start}}^{T_{end}} dt \cdot t\Delta R_2(t)}{\int_{T_{start}}^{T_{end}} dt \cdot \Delta R_2(t)} \quad (2)$$

where T_{start} was the starting time of the first pass of contrast medium in each pixel and T_{end} was the ending time. The relative CBF (rCBF) was obtained as *rCBV/rMTT*. Our third analysis was based on what we call the FIX method. The analysis was performed by measuring the mean start time and end time of the bolus passage of contrast medium in the entire brain and then applying the values to each pixel to measure parameters as the first-pass-start time and first-pass-end time, respectively. The equations to generate rCBV and rMTT were the same as those used in the PIX method. Having generally witnessed good correlations between FIX results and PET results in the past, we decided to include the former in this study. All the generated maps were filtered with a 5-mm full-width at half-maximum (FWHM) to achieve a resolution similar to that of the PET maps.

Positron Emission Tomography Study with ^{15}O Gases

The method used for our PET study has been described previously (Nariai *et al*, 1994). Briefly, the PET study was performed using a Headtome-V scanner (Shimadzu Corporation, Kyoto, Japan). The regional CBF and OEF were measured during continuous and consecutive 9-min inhalations of $C^{15}O_2$ and $^{15}O_2$ with continuous arterial blood sampling, employing a table-lookup technique (Senda *et al*, 1988). The regional CBF and OEF were obtained by calculating the values with lookup tables created from the arterial whole blood and plasma radioactivity curves, and then correcting them for delay and dispersion (Iida *et al*, 1986). The CBV was measured by a 3-min inhalation of $C^{15}O$ with blood sampling (Grubb *et al*, 1978). The OEF was corrected for the effect of the regional CBV (Lammertsma and Jones, 1983; Mintun *et al*, 1984). The MTT was calculated as *CBV/CBF*. All the PET images were reconstructed into a series of seven 5-mm-thick axial images with 7.5-mm intergaps, matched to the PWI level in each patient to set the regions of interests (ROIs) for PET and PWI in the same locations.

Analysis by Placing Region of Interests and Statistics

Abnormalities of cerebral hemodynamics in each patient were evaluated by manually placing the ROIs over the cerebral cortex (frontal, temporal parietal, and sensorimotor cortex) supplied by the internal carotid system (anterior circulation) and the upper cortex of the cerebellum, avoiding the infarcted area. Each ROI consisted of a series of 1-cm-diameter circles along the cortical rim. The mean values of MTT or rMTT, rCBF or CBF, and CBV or rCBV of the ROIs in each hemisphere were calculated (anterior MTT, anterior CBF, and anterior CBV, respectively) for both PWI and PET. In the PWI data, we also calculated the ratios of the anterior CBF (CBF ratio) and anterior CBV (CBV ratio) to the cerebellum. The corresponding data between the PWI and PET of CBF (PWI–CBF ratio versus PET–anterior CBF), CBV (PWI–CBV ratio versus PET–anterior CBV), and MTT (PWI–anterior MTT versus PET–anterior MTT) were compared with each other. The delay of the anterior MTT compared with the MTT or rMTT of the cerebellum measured by PWI was termed the 'MTT delay' and examined for correlations with the OEF and CBV obtained by PET.

All the data were expressed as mean $\pm$ s.d. Spearman's test and linear regression analysis were used to assess correlations between PWI and PET parameter values of the CBF ratio, CBV ratio, and anterior MTT. Correlations of the MTT delay of PWI with the OEF ratio and CBV from PET measurements were statistically analyzed by various regressions. Cluster analysis by the *K*-mean method was also applied to analyze the distribution of pixel values between PWI and PET. A *P*-value of <0.05 was considered statistically significant throughout the study.

Results

General Findings

Both PET and PWI data showed various hemodynamic abnormalities in unilateral or bilateral hemispheres in all of the patients studied. Yet, a comparison between the images obtained by the two methods clearly illustrated that only PWI could provide regional information on a gyrus-by-gyrus level (see Figure 1). Perfusion-weighted magnetic resonance imaging could be directly compared with morphological MRI, allowing the direct detection of abnormalities in CBF, CBV, and MTT on a precise anatomical basis. Perfusion-weighted magnetic resonance imaging could also be performed rapidly, with an acquisition time only 60 secs longer than that of a conventional MRI examination. Positron emission tomography, in contrast, took more time and required registration process with morphological images (Nariai *et al*, 1997; Shimada *et al*, 2000). The high spatial resolution of the MR perfusion maps was more useful for regional evaluation than the lower resolution of the PET images (Figure 1).

Correlation Between Magnetic Resonance Imaging and Positron Emission Tomography-Measured Cerebral Blood Flow, Cerebral Blood Volume, and Mean Transit Time

The correlations between PWI data and PET data on CBF, CBV, and MTT are illustrated in Figure 2. All CBV and MTT measurement variables calculated by the three analytic methods corresponded signifi-

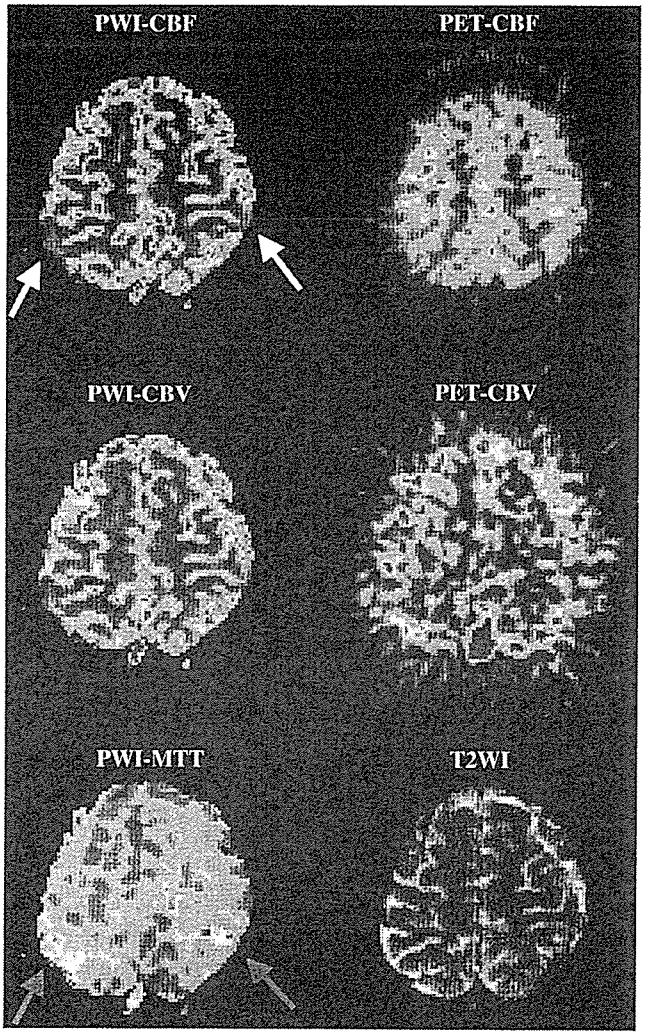

Figure 1 Parametric maps to indicate CBF and CBV obtained by PWI (Fix method) and PET in a 35-year-old woman with moyamoya disease. The MTT map of PWI is also shown. The CBF–PWI map indicated a decrease in CBF in the bilateral parietal regions (white arrows). The MTT-PWI map indicated MTT prolongation in the same regions (red arrows). The regional distribution of CBF and CBV detected by PWI correlated well with that detected by PET, but the spatial resolution of the former was far better than that of the latter.

cantly with the PET data. The CBV ratio obtained by the PIX method had the highest correlation with the PET-measured CBV value ($R^2 = 0.58$, $P < 0.01$, with the PIX method) among the three methods, and the ratios determined by the PIX and FIX analytic methods in the MTT measurement correlated well with the PET data ($R^2 = 0.58$, $P < 0.01$, with the PIX method; $R^2 = 0.67$, $P < 0.01$, with the FIX method). However, the only association between the PW1-measured CBF and PET-measured CBF was a weak but less than significant correlation determined by the FIX method ($R^2 = 0.06$, $P = 0.06$). Based on these results, variables applied by PIX and FIX methods were used for further analysis.

Detection of Misery Perfusion Using Perfusion-Weighted Magnetic Resonance Imaging

While the MTT has been used as an index of reduced cerebral perfusion pressure (Gibbs *et al*, 1984), an MTT prolonged beyond normal (i.e., reduced perfusion pressure) does not necessary lead to a reduced CBF. The compensatory mechanism to increase the focal vascular bed works well to preserve CBF until the reduction of perfusion pressure exceeds a certain threshold. This threshold is thought to correspond to the border between grade 1 and 2 hemodynamic stress, as defined by Powers *et al* (Powers, 1991; Powers *et al*, 1987). As MTT is theoretically considered a reciprocal of perfusion pressure, we might be able to detect grade 2 hemodynamic stress (misery perfusion) by defining the threshold of MTT prolongation.

In our comparison between PWI-MTT and PET-OEF on the parametric image maps, the areas with highly prolonged MTT closely corresponded with the areas with elevated OEF measured by PET (Figure 3). We therefore plotted the PET-measured OEF (ratio to control) against the MTT (MTT delay) measured by the PIX and FIX methods in the PWI analysis. Correlations between the MTT delay obtained by the PIX method and the OEF ratio obtained by PET were slightly better fit by quadratic correlation ($R^2 = 0.61$, $P < 0.001$) than by linear correlation ($R^2 = 0.57$, $P < 0.001$). Correlations between the MTT delay obtained by the FIX method and the OEF ratio obtained by PET were lower than that obtained by PIX method (quadratic correlation, $R^2 = 0.46$, $P < 0.001$; linear correlation, $R^2 = 0.43$, $P < 0.001$). Thus, the MTT delay calculated by the PIX method was used for further analysis (Figure 4). We statistically clustered the distribution of pixels into two categories by the *K*-mean method, as shown in the graph in Figure 4B. This figure clearly indicates the division of the pixels into normal OEF and abnormally elevated OEF using an MTT delay of 2.0 secs as a threshold. In the cerebral hemispheres where the MTT delay was within 2 secs, the OEF value did not exceed 120% of control. When the MTT delay exceeded 2 secs, however, the OEF value rose in proportion to the MTT delay. This suggests that the presence and grade of misery perfusion might be detectable by measuring the MTT delay with PWI.

In our examination of the relationship between the MTT delay by the PIX method and the CBV measured by PET, the latter tended to rise gradually in proportion to the duration of the MTT delay up to a delay of about 2.0 secs (Figure 4C). In the highly prolonged range, however, the CBV remained stably at around the 6 mL/100 g level irrespective of the duration of the MTT delay. The correlation between the MTT delay obtained by the PIX method on MRI and the CBV obtained by PET was slightly better fit by negative quadratic correlation ($R^2 = 0.34$, $P < 0.001$) than by linear correlation ($R^2 = 0.31$,

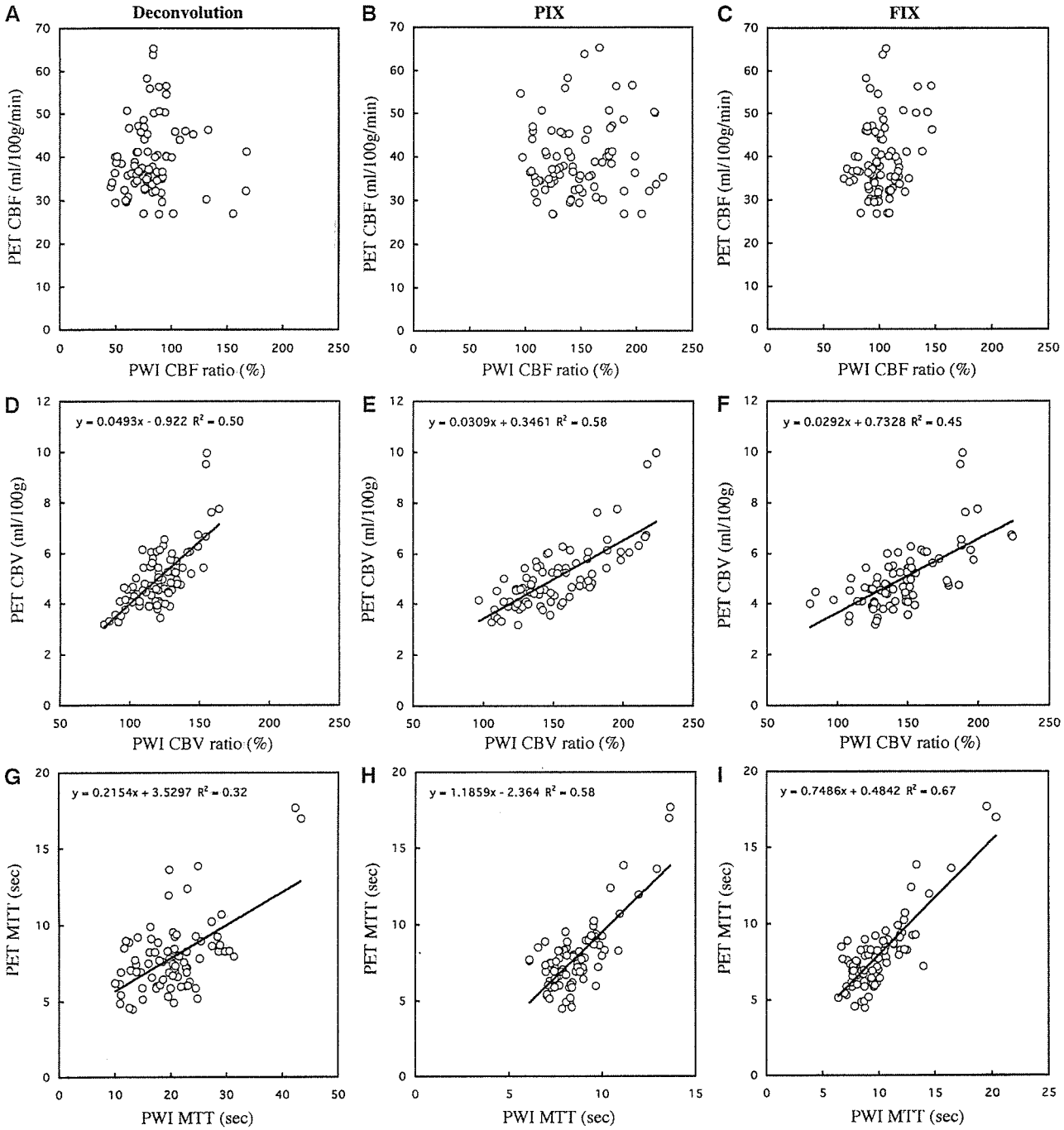

Figure 2 Correlation between PWI and PET measurements of CBF (**A–C**), CBV (**D–F**), and MTT (**G–I**). The correlation coefficient (R^2) obtained in each analysis is also displayed in each graph. All the CBV and MTT data generated by three methods were significantly correlated with CBV and MTT findings obtained by PET, respectively. There were no significant correlations between PWI and PET measurements of CBF (regression curve not shown).

$P<0.001$). By clustering the pixels into two categories, we could differentiate the dimension with prolonged MTT and elevated CBV from that with only moderate abnormalities of the two parameters (Figure 4D). Clustering on the *x*-axis was not as clearly depicted as it was in the case of OEF, but the MTT delay of 1.5 to 2.0 secs could be used as a divider.

Before applying the threshold MTT delay value in actual clinical decision-making, we need to ascertain its sensitivity and specificity in detecting abnormally elevated OEF and CBV using the 2-sec MTT delay as a threshold. We did this by calculating the sensitivity and specificity of the method in detecting the mean + 2s.d. of the OEF ratio to the cerebellum and CBV using normal control data from

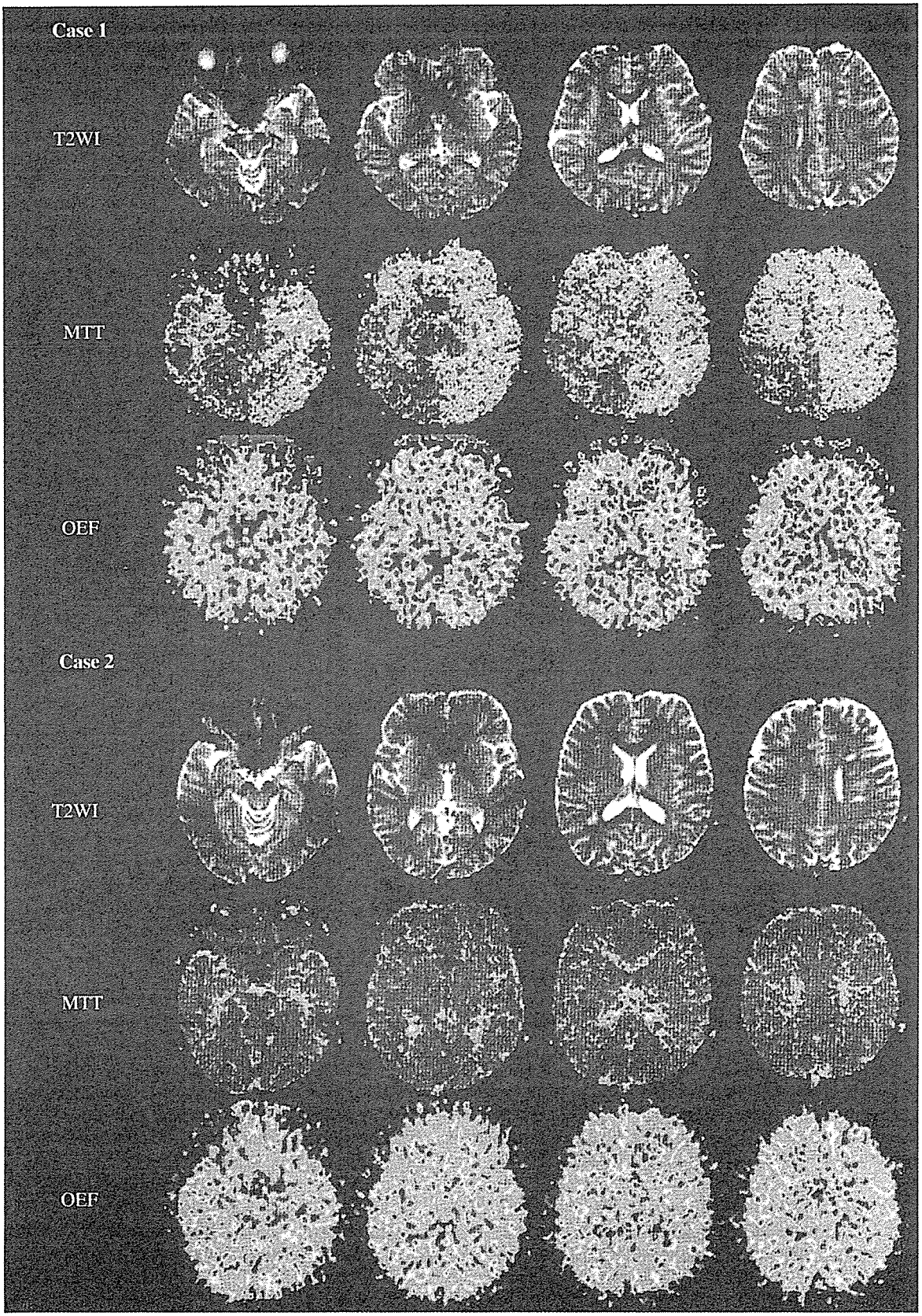
Case 1
T2WI
MTT
OEF
Case 2
T2WI
MTT
OEF

our earlier study (Nariai *et al*, 2005). Lines to indicate these threshold values are displayed in Figures 4B and 4D. Through the calculation with these values, we determined that the threshold MTT delay value of 2.0 secs had a sensitivity and specificity of 92.3% (12/13) and 100% (12/12) in detecting regions with abnormally elevated OEF ratio, and 20.0% (12/60) and 100% (12/12) in detecting regions with abnormally elevated CBV, respectively.

Discussion

In the present report, we used data from moyamoya patients to analyze whether the hemodynamic parameters obtained with PWI are reliable for use in clinical decision-making in the treatment of patients with chronic occlusive cerebrovascular disease.

In making clinical decisions in the treatment of patients with occlusive cerebrovascular disease, it is

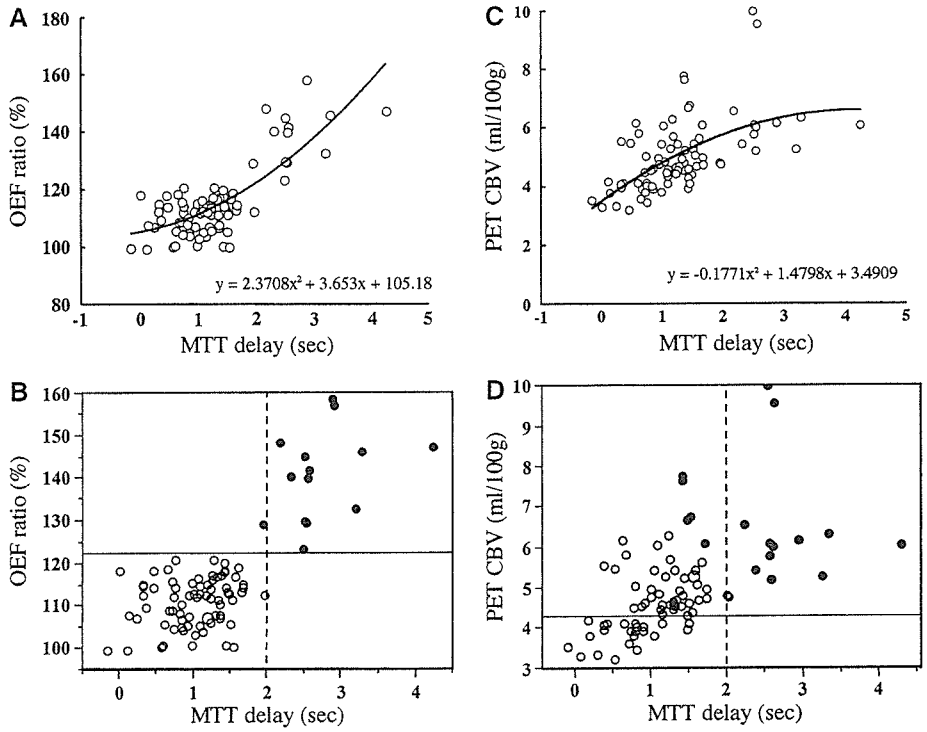

Figure 4 (**A**, **B**) show the correlation between the delay of PWI-MTT compared with the cerebellum (*x*-axis), and the PET-OEF ratio with the cerebellum (*y*-axis). The upper graph (**A**) shows the results of the regression analysis. The quadratic polynomial fits better than the linear polynomial, as indicated in the text. The lower graph (**B**) shows the results of cluster analysis by the *K*-mean method. The area with MTT delay of more than 2.0 secs shows an unmistakable elevation of OEF (indicated with black dots). The dotted vertical line indicates a 2.0-sec MTT delay and the horizontal solid line indicates the mean + 2s.d. of the OEF ratio among normal controls (121.7%). Using these values, the sensitivity and specificity in detecting the regions with abnormally elevated OEF ratios were calculated as 92.3% and 100%, respectively. (**C**, **D**) show the correlation between the delay of PWI-MTT compared with the cerebellum (*x*-axis) and PET-CBV (*y*-axis). The upper graph (**C**) shows the results of regression analysis. The quadratic polynomial fit better than the linear polynomial, as indicated in the text. The lower graph (**D**) shows the results of cluster analysis by the *K*-mean method. This graph indicates that the area with MTT delay of more than 2.0 secs comprised a group of regions with maximally elevated CBV (indicated with black dots). The dotted vertical line indicates a 2.0-sec MTT delay and the horizontal solid line indicates the mean + 2s.d. of CBV among normal controls (4.27). Using these values, the sensitivity and specificity in detecting the regions with abnormally elevated CBV were calculated as 20% and 100%, respectively. Perfusion-weighted imaging data was generated by the PIX method.

Figure 3 T2-weighted MRI (T2WI) (upper row), parametric maps to indicate MTT obtained with PWI (MTT) (middle row) and OEF images obtained with PET (lower row) of two representative moyamoya patients. Conventional MRI of case 1, a 26-year-old woman suffering from frequent temporary ischemic attacks (TIAs), depicted an infarcted area in the left frontal lobe. A parametric map of MTT showed a severe prolongation of transit time in the left entire hemisphere and right frontal lobe, and these findings closely corresponded with the OEF-elevated area. Case 2 was a 42-year-old woman who had been diagnosed with moyamoya disease incidentally and had no history of ischemic episodes. An infarcted area was also detected in the left frontal lobe, but the MTT map revealed almost normal circulation time in the entire brain. The parametric map of OEF also presented no abnormal elevation. MTT, mean transit time; OEF, oxygen extraction fraction; T2WI, echo-planar T2-weighted image.

now considered important to ascertain the degree of hemodynamic stress to predict the patient outcome (Derdeyn *et al,* 2002; Grubb *et al,* 1998). Simultaneous PET measurement of CBF and metabolism is the only known way to confirm the established risk factors (elevated OEF, misery perfusion, grade 2 hemodynamic stress). But rather than offering information of physiological significance, elevated OEF merely tells us that the decrease in focal perfusion pressure exceeds the maximum limit of the compensatory mechanism to increase the vascular bed for the preservation of CBF. As MTT measured by PWI is theoretically considered a reciprocal of perfusion pressure, we speculated that a comparison between PWI-measured MTT and PET-measured OEF may provide information useful for the detection of grade 2 hemodynamic stress.

In our analysis presented in Figure 4, OEF remained largely unchanged until the MTT delay in the anterior circulation of the cerebral hemisphere reached approximately 2 secs, whereupon it increased in proportion to the MTT delay beyond the 2-sec level. In our comparison of the CBV value from PET and the MTT value from the PIX method, however, the CBV showed no apparent increase once the MTT delay reached approximately 1.5–2.0 secs. The pixels were statistically clustered into two categories in both plots: pixels with only moderately prolonged MTT with normal OEF and moderately increased CBV, and pixels with markedly prolonged MTT with abnormally elevated OEF and saturated CBV.

By interpreting these plots with the theoretical consideration of the compensatory mechanism against major vessel occlusion proposed by Powers *et al* (Powers, 1991; Powers *et al,* 1987), we can align the threshold of the perfusion delay with the limit of vasodilatation to keep the CBF. In other words, we can detect the border between grade 1 and grade 2 hemodynamic stress at the threshold MTT delay value of around 2.0 secs, and the area with delay exceeding this point can be assumed to represent a state of misery perfusion. The analysis of sensitivity and specificity to detect abnormal OEF and CBV using this threshold value in Figure 4 also supports this assumption. High sensitivity and high specificity in detecting the region with elevated OEF indicate high reliability of the threshold MTT delay value to detect the border between grade 1 and grade 2. However, the low sensitivity of the 2.0-sec MTT delay in detecting the elevated CBV tells us that the CBV is already elevated before the MTT delay reaches 2.0 secs, without any corresponding elevation of OEF. This means, in turn, that the hemodynamic stress falls within the grade 1 range when the MTT delay remains less than 2.0 secs. Moreover, the 100% specificity of the more than 2 secs MTT delay in detecting elevated CBV tells us that grade 2 hemodynamic stress is always accompanied by elevated CBV. While several reports have investigated the use of PWI for the analysis of perfusion deficit (Baird and Warach, 1998; Maeda *et al,* 1999; Warach *et al,* 1996) and the loss of cerebrovascular reserve capacity (Schreiber *et al,* 1998) based on the MTT delay, no reports have interpreted the usefulness of the perfusion delay in depicting critical points for the prediction of misery perfusion. Our success in detecting this critical point by PWI in the present study may relate to the characteristics of moyamoya disease.

Moyamoya disease is a slowly progressive cerebrovascular disease which characteristically manifests variable degrees of perfusion deficit (Nariai *et al,* 2005). This variability in perfusion deficit makes the disease a suitable subject for comparative study using multiple modalities. However, our present results may also provide valuable insight into the specific pathophysiology of moyamoya disease. The application of PWI in cases with moyamoya disease has already been reported (Calamante *et al,* 2001; Kassner *et al,* 2003; Lee *et al,* 2003; Tsuchiya *et al,* 1998; Yamada *et al,* 1999). However, no studies have fully evaluated the accuracy of PWI measurement in moyamoya disease patients through comparisons with quantitative data acquired by other modalities, such as PET. Moyamoya disease usually exhibits a specific cerebral circulation pattern through leptomeningeal collaterals, and the focal perfusion is generally highly delayed. Thus, PWI and other methods to detect the bolus passage of contrast media are probably heavily affected by delay and dispersion (Calamante *et al,* 2000; Wu *et al,* 2003). Our result suggested that PWI potentially has the same level of reliability as PET in the quantitative measurement of CBV and MTT. Given the considerable scatter seen in the plots of Figure 2, however, caution should be taken in using this method for clinical decision-making. Henceforth, we will need to conduct ongoing comparative studies between PWI and PET to confirm the clinical reliability. Studies comparing the PWI parameters with clinical symptoms and treatment courses in individual patients with moyamoya disease will also be needed to confirm the utility of PWI measurement in the daily clinical setting.

In contrast to the PWI measurements of MTT and CBV and their promising utility, none of the three analysis methods using PWI showed any correlation with CBF measured by PET. We attributed this to the larger errors generated in the calculation of CBF due to the measurement errors of CBV and MTT in the PIX method. We also noted that the deconvolution method seemed to skew the CBF values. Further, the poor reliability of the AIF obtained from the internal carotid arteries already manifesting the lesional changes of the type seen in most patients with moyamoya disease hampers the accurate assessment of CBF by the AIF method.

Arterial spin-labeling (ASL) might have promise as an alternative method for evaluating CBF quantitatively. It should be noted, however, that ASL methods such as flow-sensitive alternating

inversion recovery (FAIR) can also be affected by the delay of the labeled spin passage (Calamante *et al*, 2001; Kim, 1995). Due to the specific circulation pattern of moyamoya disease, the transit time is prolonged and the FAIR technique is unable to differentiate between very long transit times and no flow (CBF = 0, no signal in the arterial spin labeling image).

As discussed above, our present analysis might be strongly influenced by the specific circulation pattern of moyamoya disease. To examine whether the same approach can be applied in other types of cerebrovascular disorder, we need to perform further comparative studies between PWI and PET with expanded populations of study candidates. Further research on the moyamoya patients from the present study is now underway to determine the correlations between the clinical features of the disease and the MTT delay measured in our current results. We are also currently conducting a prospective observation of both surgically and medically treated patients based on PWI data. These further analyses will better clarify the utility and limitations of PWI for clinical application.

In conclusion, PWI measurement provided sufficient quantitative evaluations of CBV and MTT in moyamoya patients. The measurement of CBF had limitations, however. Among the various parameters investigated, our results suggested that the duration of MTT delay might be used to detect the presence and degree of misery perfusion.

References

Baird AE, Warach S (1998) Magnetic resonance imaging of acute stroke. *J Cereb Blood Flow Metab* 18:583–609

Calamante F, Gadian DG, Connelly A (2000) Delay and dispersion effects in dynamic susceptibility contrast MRI: simulations using singular value decomposition. *Magn Reson Med* 44:466–73

Calamante F, Ganesan V, Kirkham FJ, Jan W, Chong WK, Gadian DG, Connelly A (2001) MR perfusion imaging in moyamoya syndrome: potential implications for clinical evaluation of occlusive cerebrovascular disease. *Stroke* 32:2810–6

Derdeyn CP, Videen TO, Yundt KD, Fritsch SM, Carpenter DA, Grubb RL, Powers WJ (2002) Variability of cerebral blood volume and oxygen extraction: stages of cerebral haemodynamic impairment revisited. *Brain* 125: 595–607

Gibbs JM, Leenders KL, Wise RJ, Jones T (1984) Evaluation of cerebral perfusion reserve in patients with carotid-artery occlusion. *Lancet* 1:182–6

Grubb RL, Jr, Derdeyn CP, Fritsch SM, Carpenter DA, Yundt KD, Videen TO, Spitznagel EL, Powers WJ (1998) Importance of hemodynamic factors in the prognosis of symptomatic carotid occlusion. *JAMA* 280:1055–60

Grubb RL, Jr, Raichle ME, Higgins CS, Eichling JO (1978) Measurement of regional cerebral blood volume by emission tomography. *Ann Neurol* 4:322–8

Iida H, Kanno I, Miura S, Murakami M, Takahashi K, Uemura K (1986) Error analysis of a quantitative cerebral blood flow measurement using H2(15)O autoradiography and positron emission tomography, with respect to the dispersion of the input function. *J Cereb Blood Flow Metab* 6:536–45

Ikezaki K, Matsushima T, Kuwabara Y, Suzuki SO, Nomura T, Fukui M (1994) Cerebral circulation and oxygen metabolism in childhood moyamoya disease: a perioperative positron emission tomography study. *J Neurosurg* 81:843–50

Kassner A, Zhu XP, Li KL, Jackson A (2003) Neoangiogenesis in association with moyamoya syndrome shown by estimation of relative recirculation based on dynamic contrast-enhanced MR images. *Am J Neuroradiol* 24:810–8

Kim SG (1995) Quantification of relative cerebral blood flow change by flow-sensitive alternating inversion recovery (FAIR) technique: application to functional mapping. *Magn Reson Med* 34:293–301

Lammertsma AA, Jones T (1983) Correction for the presence of intravascular oxygen-15 in the steady-state technique for measuring regional oxygen extraction ratio in the brain: 1. Description of the method. *J Cereb Blood Flow Metab* 3:416–24

Lee SK, Kim DI, Jeong EK, Kim SY, Kim SH, In YK, Kim DS, Choi JU (2003) Postoperative evaluation of moyamoya disease with perfusion-weighted MR imaging: initial experience. *Am J Neuroradiol* 24:741–7

Maeda M, Yuh WT, Ueda T, Maley JE, Crosby DL, Zhu MW, Magnotta VA (1999) Severe occlusive carotid artery disease: hemodynamic assessment by MR perfusion imaging in symptomatic patients. *Am J Neuroradiol* 20:43–51

Matsushima Y (1999) Moyamoya disease. In: *Principle and Practice of Pediatric Neurosurgery* (Albright A, Pollack I, Adelson P, eds), New York: Thieme, 1053–69

Mintun MA, Raichle ME, Martin WR, Herscovitch P (1984) Brain oxygen utilization measured with O-15 radiotracers and positron emission tomography. *J Nucl Med* 25:177–87

Nariai T, Matsushima Y, Imae S, Tanaka Y, Ishii K, Senda M, Ohno K (2005) Severe hemodynamic stress in selected subtypes of patients with moyamoya disease—a positron emission tomography study. *J Neurol Neurosurg Psychiatry* 76:663–9

Nariai T, Senda M, Ishii K, Maehara T, Wakabayashi S, Toyama H, Ishiwata K, Hirakawa K (1997) Three-dimensional imaging of cortical structure, function and glioma for tumor resection. *J Nucl Med* 38:1563–8

Nariai T, Suzuki R, Hirakawa K, Maehara T, Ishii K, Senda M (1995) Vascular reserve in chronic cerebral ischemia measured by the acetazolamide challenge test: comparison with positron emission tomography. *Am J Neuroradiol* 16:563–70

Nariai T, Suzuki R, Matsushima Y, Ichimura K, Hirakawa K, Ishii K, Senda M (1994) Surgically induced angiogenesis to compensate for hemodynamic cerebral ischemia. *Stroke* 25:1014–21

Ostergaard L, Johannsen P, Host-Poulsen P, Vestergaard-Poulsen P, Asboe H, Gee AD, Hansen SB, Cold GE, Gjedde A, Gyldensted C (1998*a*) Cerebral blood flow measurements by magnetic resonance imaging bolus tracking: comparison with [(15)O]H_2O positron emission tomography in humans. *J Cereb Blood Flow Metab* 18:935–40

Ostergaard L, Smith DF, Vestergaard-Poulsen P, Hansen SB, Gee AD, Gjedde A, Gyldensted C (1998*b*) Absolute cerebral blood flow and blood volume measured by